A revision of the early neotheropod genus **Sarcosaurus** from the Early Jurassic (Hettangian–Sinemurian) of central England

Ezcurra, Martin; Butler, Richard; Maidment, Susannah; Sansom, Ivan; Meade, Luke; Radley, Jonathan

DOI:
10.1093/zoolinnean/zlaa054

A revision of the early neotheropod genus *Sarcosaurus* from the Early Jurassic (Hettangian–Sinemurian) of central England

Martín D. Ezcurra[1,2]*, Richard J. Butler[2], Susannah C. R. Maidment[2,3], Ivan J. Sansom[2], Luke E. Meade[2] and Jonathan D. Radley[2]

[1] *Sección Paleontología de Vertebrados, CONICET-Museo Argentino de Ciencias Naturales, Ángel Gallardo 470, C1405DJR, Buenos Aires, Argentina*

[2] *School of Geography, Earth and Environmental Sciences, University of Birmingham, Edgbaston, Birmingham B15 2TT, UK*

[3] *Department of Earth Sciences, Natural History Museum, Cromwell Road, London SW7 5BD, UK*

* *Corresponding author: martindezcurra@yahoo.com.ar*

Running title: Revision of the Jurassic theropod *Sarcosaurus*

Abstract. Neotheropoda represents the main evolutionary radiation of predatory dinosaurs and its oldest records come from Upper Triassic rocks (ca. 219 Mya). The Early Jurassic record of Neotheropoda is taxonomically richer and geographically more widespread than that of the Late Triassic. The Lower Jurassic (upper Hettangian–lower Sinemurian) rocks of central England have yielded three neotheropod specimens that have been assigned to two species within the genus *Sarcosaurus*, *S. woodi* (type species) and *S. andrewsi*. These species have received little attention in discussions of the early evolution of Neotheropoda, and recently have been considered as *nomina dubia*. Here, we provide a detailed redescription of one of these specimens (WARMS G667–690) and reassess the taxonomy and phylogenetic

relationships of the genus *Sarcosaurus*. We propose that the three neotheropod specimens from the Early Jurassic of central England represent a single valid species, *S. woodi*., ~~, and~~ Tthe second species of the genus, '*S. andrewsi*', is a subjective junior synonym of the former. A quantitative phylogenetic analysis of early theropods recovered *S. woodi* as one of the closest sister taxa to Averostra and provides new information on the sequence of character-state transformations in the lead up to the phylogenetic split between Ceratosauria and Tetanurae.

Key words: Dinosauria, Theropoda, Coelophysoidea, Averostra, phylogeny, Europe

INTRODUCTION

The oldest known dinosaurs come from Upper Triassic continental rocks in South America, dated to approximately 233–231 Mya, and probably coeval strata in Africa and India (Rogers *et al.*, 1993; Furin *et al.*, 2006; Langer, Ramezani & Da Rosa, 2018). These first recorded dinosaurs include some predatory forms, such as the early theropod *Eodromaeus murphi* Martinez *et al.*, 2011 and the herrerasaurids (alternatively interpreted as early theropods or non-eusaurischian saurischians; e.g. Langer & Benton, 2006; Nesbitt *et al.*, 2009; Martínez *et al.*, 2011). However, the main evolutionary radiation of predatory dinosaurs is represented by Neotheropoda, the oldest records of which (*Camposaurus arizonensis*: Hunt *et al.*, 1998;; Ezcurra & Brusatte, 2011; *Lepidus praecisio*: Nesbitt & Ezcurra, 2015) come from rocks of the southwestern USA dated to 219.39 ± 0.16 Mya (Ramezani *et al.*, 2014; Marsh *et al.*, 2019a) or older (Nesbitt & Ezcurra, 2015). Younger Triassic neotheropods are unambiguously restricted to middle Norian to probably Rhaetian beds of Argentina (Arcucci & Coria, 2003; Ezcurra, 2017; Martínez & Apaldetti, 2017), USA (e.g. Cope, 1889; Padian, 1986; Colbert, 1989; Carpenter, 1997), Europe (Fraas, 1913; Jaekel, 1913; Huene, 1932, 1934; Rauhut & Hungerbühler, 2000; Dzik, Sulej & Niedźwiedzki, 2008) and India (Novas *et al.*, 2010). By contrast, the Early Jurassic record of Neotheropoda is taxonomically richer and geographically more widespread, with multiple known species and occurrences on all continents with the exception of Australia (e.g. Woodward, 1908; Talbot, 1911; Andrews, 1921; Huene, 1932; Camp, 1936; Young, 1948; Welles, 1954; Raath, 1969; Yadagiri, 1982; Rowe, 1989; Hu, 1993; Hammer & Hickerson, 1994; Benton, Martill & Taylor, 1995; Lucas & Heckert, 2001; Irmis, 2004; Yates, 2005; Munter & Clark, 2006; Allain *et al.*, 2007; Delsate & Ezcurra, 2014; Langer *et al.*, 2014; You *et al.*, 2014; Martill *et al.*, 2016; Wang *et al.*, 2017a; Dal Sasso, Maganuco & Cau, 2018).

The Lower Jurassic rocks of central England have yielded three neotheropod specimens that, although rather incomplete, were the best records of the group from this time interval in the UK (Huene, 1932; Carrano & Sampson, 2004), prior to the recent discovery of *Dracoraptor hanigani* (Martill *et al.,* 2016). Andrews (1921) described a fragmentary theropod specimen collected from the lower part of the Lias Group (*bucklandi* zone, lower Sinemurian) of Barrow upon Soar in Leicestershire (Fig. 1). This specimen, NHMUK PV R4840 includes a partial posterior dorsal vertebra, pelvis, and left femur. Andrews (1921) made this specimen the type species of a new genus and species, *Sarcosaurus woodi* Andrews, 1921. The taxon has received little subsequent attention, but was reviewed and redescribed by Carrano & Sampson (2004), who referred it to Coelophysoidea. They argued that *Sarcosaurus woodi* was likely to be distinct from all other known taxa based on its provenance, but considered it as a *nomen dubium* because they were unable to diagnose the species based on either autapomorphies or a distinct combination of character states.

Two additional Lias Group theropod specimens were described from Wilmcote in Warwickshire (Fig. 1). Woodward (1908) described NHMUK PV R3542, a right tibia, from the late Hettangian *angulata* zone. Huene (1932) subsequently made this specimen the type of the new species, *Sarcosaurus andrewsi* Huene, 1932, which was also considered a *nomen dubium* by Carrano & Sampson (2004). Huene (1932) also described a fragmentary partial skeleton, WARMS G667–690 (Fig. 2), which he referred to *Sarcosaurus woodi*. This material was briefly discussed by Carrano & Sampson (2004), who identified it as cf. *Sarcosaurus woodi*, but without providing a full redescription or figuring any of the material.

Here, we provide a detailed redescription of WARMS G667–690, which, although fragmentary, represents one of the most complete theropod specimens known from the Lower Jurassic of the UK. We review the taxonomy of all three specimens that have been referred to

the genus *Sarcosaurus*, and assess their phylogenetic positions in an analysis of early theropod dinosaurs.

INSTITUTIONAL ABBREVIATIONS

AMNH, American Museum of Natural History, New York, USA; CM, Carnegie Museum of Natural History, Pittsburg, Pennsylvania, USA; IVIC, Colección Paleontológica del Centro de Ecología, Instituto Venezolano de Investigaciones Científicas, Caracas, Venezuela; LPRP/USP, Laboratório de Paleontologia de Ribeirão Preto, Universidade de São Paulo, Ribeirão Preto, Brazil; MACN-Pv CH, Museo Argentino de Ciencias Naturales 'Bernardino Rivadavia', Paleovertebrados, Colección Chubut, Buenos Aires, Argentina; HMN, Museum für Naturkunde der Humboldt Universität, Berlin, Germany; MCZ, Museum of Comparative Zoology, Cambridge, USA; MNA, Museum of Northern Arizona, Flagstaff, USA; MPEF, Museo Paleontológico Egidio Feruglio, Trelew, Argentina; NHMUK PV, The Natural History Museum, Palaeontology Vertebrates, London, UK; NMW, National Museum of Wales, Cardiff, UK; PULR, Paleontología, Universidad Nacional de La Rioja, La Rioja, Argentina; PVL, Paleontología de Vertebrados, Instituto 'Miguel Lillo', San Miguel de Tucumán, Argentina; PVSJ, División de Paleontología de Vertebrados del Museo de Ciencias Naturales y Universidad Nacional de San Juan, San Juan, Argentina; QG, Zimbabwe Natural History Museum, Bulawayo, Zimbabwe; SMNS, Staatliches Museum für Naturkunde Stuttgart, Stuttgart, Germany; UCM, University of Colorado Museum, Boulder, Colorado, USA; UCMP, University of California Museum of Paleontology, Berkeley, CA, USA; USNM, National Museum of Natural History (formerly United States National Museum), Smithsonian Institution, Washington, D.C., USA; WARMS, Warwickshire Museum, Warwick, UK.

MATERIALS AND METHODS

PHYLOGENETIC ANALYSIS

The phylogenetic relationships of the three Early Jurassic neotheropod specimens from central England were tested using the phylogenetic dataset originally published by Nesbitt *et al.* (2009) and iteratively modified by Ezcurra & Brusatte (2011), You *et al.* (2014), Nesbitt & Ezcurra (2015), Martill *et al.* (2016), Ezcurra (2017), Martínez & Apaldetti (2017), Marsola *et al.* (2019), Marsh *et al.* (2019b)~~,~~ and Griffin (2019) (Supporting Information I). Here, WARMS G667–690 and the holotypes and only known specimens of *Sarcosaurus andrewsi* and *Sarcosaurus woodi* were added to the data~~-~~set. In addition, *Tachiraptor admirabilis* Langer *et al.*, 2014 and the early ceratosaurian *Eoabelisaurus mefi* Pol & Rauhut, 2012 were added to improve the sampling of early members of the lineage leading to Averostra and early averostrans, respectively ~~(Pol & Rauhut, 2012; Langer *et al.*, 2014)~~. These specimens/species were scored based on first-hand observations of specimens (casts in the case of *Tachiraptor admirabilis*: LPRP/USP 0747, cast of IVIC-P-2867~~,~~; and *Gojirasaurus quayi* Carpenter, 1997: HMN MB.R. 4232.1, cast of UCM 47221). Five characters were added to this data matrix, character 252 was deactivated, and some character formulations, scorings and orderings were modified (rationale for these changes is given in Supporting Information I). '*Powellvenator podocitus* holotype' and '*Lepidus praecisio* combined' were deactivated before the analyses, whereas *Powellvenator podocitus* Ezcurra, 2017 and '*Lepidus praecisio* holotype' remained active following Ezcurra (2017). *Velociraptor mongoliensis* Osborn, 1924 was also deactivated following Ezcurra (2017). The resulting matrix consists of 379 characters and 57 active terminals (Supporting Information II and III). *Sarcosaurus woodi*, WARMS G667–690 and *Sarcosaurus andrewsi* were analysed in separate analyses as ~~separate~~ independent terminals or alternatively merged into a single

terminal following the hypothesis that they belong to the same species (see below).

The outgroup choice follows Nesbitt *et al.* (2009) and the following multistate characters were ordered: 17, 30, 67, 128, 129, 174, 184, 197, 213, 219, 231, 236, 248, 253, 254, 273, 329, 343, 345, 347, 349, 354, 366, 371, 374~~,~~ and 377–379. The data matrix was analysed under equally weighted parsimony using TNT 1.5 (Goloboff, Farris & Nixon, 2008; Goloboff & Catalano, 2016). A heuristic search of 100 replications of Wagner trees (with random addition sequence) followed by TBR branch swapping (holding ~~10~~ ten trees per replicate) was performed. Branches with a maximum possible length of zero among any of the recovered most parsimonious trees (MPTs) were collapsed (rule 3 of Swofford & Begle, 1993; Coddington & Scharff, 1994).

As a measure of branch support, decay indices (= Bremer support) were calculated (Bremer, 1988, 1994), and as a measure of branch stability, a bootstrap resampling analysis (Felsenstein, 1985) was conducted, performing 10,000 pseudoreplications. Both absolute and GC (*i.e.*, difference between the frequency whereby the original group and the most frequent contradictory group are recovered in the pseudoreplications; Goloboff *et al.*, 2003) bootstrap frequencies are reported. In order to analyse the effect that a few topologically unstable terminals may have on Bremer supports, this index was recalculated after the *a posteriori* pruning of such terminals, which were previously detected in the subsample of suboptimal trees with the iterPCR protocol (Pol & Escapa, 2009). Finally, analyses forcing topological constraints were conducted to find the minimum number of steps necessary to force alternative suboptimal positions for the three neotheropod specimens from the Early Jurassic of central England.

THIN SECTION PROCEDURE

Doubly polished thin sections through the dorsal rib shaft were prepared, initially stabiliz~~s~~ed

using a surface impregnation of Epothin epoxy resin, before slicing using a Buehler IsoMet Low Speed Saw (model 11-1180-160). The sections were then ground and polished (with water suspended 0.3 micron alumina oxide) to a usable thickness (approximately 50 microns) by hand on a Buehler MetaServ. Imaging was undertaken on a Zeiss Axioskop Pol polarizsation microscope using plane polarizsed and polarizsed light, the latter augmented by the insertion of an accessory gypsum plate.

3D MODELS OF SPECIMENS

High-resolution 3D models were created of selected elements of WARMS G667–690 using photogrammetry. These comprised a partial dorsal vertebra (G678), the femora (G681, G682) and tibiae (G668, G680), and the partial left metatarsal II (G672). A tripod mounted Nikon D5100 digital SLR camera with a Nikon 18−55mm VR lens was used to photograph the specimens under artificial lighting against a uniformly coloured and contrasting background. A minimal aperture ensured the whole specimen was in focus and the ISO setting was kept below 400. Around 20−40 photographs were taken in a circular path around each specimen for three different orientations to ensure even and complete coverage and a sufficient total number of photographs (60−100). The software package Agisoft PhotoScan Professional edition version 1.2.7 was used to mask the backgrounds of the photographs and create 3D meshes using automated point picking and triangulation of point clouds. These surfaces were then textured in PhotoScan and exported. The final models have been published in Zenodo and can be downloaded from here: https://zenodo.org/record/3663095.

The holotypes of *Sarcosaurus woodi* (NHMUK PV R4840) and *Sarcosaurus andrewsi* (NHMUK PV R3542) were scanned using a Faro Edge laser scanner with an arm accuracy ±0.041 mm. The line module samples 560,000 points/sec with repeatability 25µm. Scans were processed in Geomagic Wrap 2017.0.2.18 64bit. Raw point data was aligned,

filtered for outliers, and a mesh generated with no noise reduction. The meshes were exported at full size and also downsampled to 20% of the vertex count. The final models are freely available and can be downloaded from the ~~Natural History Museum's~~ data portal of the Natural History Museum here: https://data.nhm.ac.uk/object/91a032f1-fd74-4464-9c37-bab839a83761/1580342400000.

STRATIGRAPHIC AND PALAEOENVIRONMENTAL CONTEXT OF WARMS G667−690

This specimen was collected from strata (*bucklandi* Zone) that were deposited in epicontinental shallow marine settings affected by sealevel fluctuations and a warm, predominantly humid climate (Simms *et al.*, 2004; Hesselbo, 2008). The *bucklandi* zone (lower Sinemurian) in south-western Warwickshire, central England (Wilmcote area; source of WARMS G667−690) is represented by the upper part of the Rugby Limestone Member (*liasicus* up to *semicosatum* zones) of the Blue Lias Formation (Ambrose, 2001). Representing typical Blue Lias lithofacies of alternating mudrocks and generally fine-grained and frequently highly fossiliferous limestones (e.g. see Old, Sumbler & Ambrose, 1987; Ambrose, 2001), the Rugby Limestone Member was deposited at a palaeolatitude of approximately 35° N in a storm-influenced offshore setting (Weedon, Jenkyns & Page, 2017). Palaeodepths in the order of at least a few tens of metres seem likely (e.g. see Hallam, 1997), below normal storm wave base (Weedon, Jenkyns & Page, 2017).

Wilmcote was situated close to the eastern margin of the Worcester Graben during the Early Jurassic, adjacent to the East Midlands Shelf (Radley, 2003). The western margin of the emergent London Platform laid approximately 60−80 km to the south-east (Donovan, Horton & Ivimey-Cook, 1979; Cox, Sumbler & Ivimey-Cook, 1999), and must have been the principle source of terrestrial biodebris (plants and sporadic vertebrate remains), found

occasionally within the Blue Lias Formation of central England (e.g. see Old, Hamblin & Ambrose, 1991).

Growing evidence for strong climatic influence on Blue Lias deposition in central England illustrates the likely mechanism for emplacement of the terrestrial WARMS G667−690 remains into an offshore shelf setting, likely from the western margin of the London Platform. Weedon, Jenkyns & Page (2017) have suggested that the more calcareous horizons (limestones and 'marls') within the Rugby Limestone Member were deposited during relatively dry, stormier conditions, involving intermittent deposition of calcareous mud as precursors of limestone beds. By contrast, the intercalated shales are equated to wetter climatic phases, involving relative stability of the water column and high clay influx from adjacent land.

Remnants of matrix on the bone surface of WARMS G667−690 are a light grey mudstone and there is no evidence of limestone matrix. The specimen was collected probably from an uncemented bed; either a calcareous mudstone or shale horizon. Either way, storm flow and/or enhanced runoff provide effective mechanisms for derivation of terrestrial reptile remains, and their introduction into a hemipelagic marine environment.

Bioerosion traces and the presence of invertebrate bioencrusters on some of the bones of WARMS G667−690 (Fig. 3) suggests that the sea floor on which the bones were ultimately buried was oxygenated, and that the remains remained free of sediment for some time prior to burial. Comparison can be made with other occurrences of bioencrusted skeletal substrates ('benthic islands' − commonly molluscan shells) present within the Rugby Limestone Member (JDR, personal observations 1999–present). Emplacement during a dryer, stormier interval seems more likely than a wetter phase, with its potential for high clay flux and benthic anoxia (Weedon, Jenkyns & Page, 2017).

SYSTEMATIC PALAEONTOLOGY

ARCHOSAURIA Cope, 1869–1870 sensu Gauthier & Padian (1985)

DINOSAURIA Owen, 1842 sensu Padian & May (1993)

THEROPODA Marsh, 1881 sensu Gauthier (1986)

NEOTHEROPODA Bakker, 1986 sensu Sereno (1998)

Sarcosaurus Andrews, 1921

Type species:

Sarcosaurus woodi Andrews, 1921.

Diagnosis:

As for type and only valid species.

Sarcosaurus woodi Andrews, 1921

Megalosaurus sp.: Huene, 1908 (NHMUK PV R3542)

Sarcosaurus sp.: Andrews, 1921 (NHMUK PV R3542)

Megalosaurus (subgenus a) sp.: Huene, 1926 (NHMUK PV R3542)

Sarcosaurus andrewsi: Huene, 1932: page 51 (NHMUK PV R3542)

Magnosaurus woodwardi: Huene, 1932: page 219 (NHMUK PV R3542)

Megalosaurus andrewsi: Waldman, 1974 (NHMUK PV R3542)

cf. *Sarcosaurus woodi*: Carrano and Sampson, 2004 (WARMS G667–690)

Holotype:

NHMUK PV R4840, a posterior dorsal vertebra, partial left and right ilia each fused to the

proximal portion of their respective pubis, and left femur missing most of the femoral head and with a severely damaged distal end.

Ontogenetic stage of holotype:

This specimen shows some indicators of skeletal maturity and is not an early juvenile, but its ontogenetic stage cannot be constrained further based on the available evidence (see Discussion).

Type locality and horizon:

Barrow upon Soar, Leicestershire, England, UK. *Bucklandi* Zz~~z~~one of the Scunthorpe Mudstone Formation, Lias Group, Early Jurassic (lowermost Sinemurian) (Fig. 1).

Referred specimens:

NHMUK PV R3542, a complete right tibia (holotype of '*Sarcosaurus andrewsi*'). WARMS G667–690, partial skeleton of a single individual (Fig. 2) including a partial middle–posterior dorsal vertebra (G678), a partial anterior–middle caudal vertebra (G679), dorsal rib fragments (G670, G675, G676, G685, G686), fragment of the pubic peduncle of the left ilium (G690), partial right and left pubes (G683/684, G688), femora (G681, G682) and tibiae (G668, G680), proximal end of left fibula (G669), probable distal half of fibula (G674), distal portions of left metatarsal II (G672), metatarsal III (G673) and metatarsal IV (G677), proximal end of a metatarsal II or III (G671), proximal half of left pedal phalanx II-1 (G687), and three indeterminate bone fragments (G680, G681, G689) (collected by J. W. Kirshaw).

Ontogenetic stage of referred specimens:

NHMUK PV R3542 is considerably larger than the other referred specimen but its

ontogenetic stage is unknown. WARMS G667–690 was not a juvenile, but had not reached skeletal maturity at the time of its death (see Discussion).

Locality and horizons of referred specimens:

Wilmcote, Warwickshire, England, UK. NHMUK PV R3542 is from the *angulata* Zone of the Blue Lias Formation, Lias Group, Early Jurassic (upper Hettangian); and WARMS G667–690 comes from the *bucklandi* Zone of the upper part of the Rugby Limestone Member of the Blue Lias Formation, Early Jurassic (lowermost Sinemurian) (Fig. 1).

Diagnosis:

Sarcosaurus woodi is a medium-sized (estimated femoral length c. 48 cm in NHMUK PV R3542) non-averostran neotheropod that differs from other dinosaurs in the following unique combination of character states present in the holotype (autapomorphies indicated with an asterisk): ilium with main axis of the preacetabular process strongly anteroventrally oriented in lateral view (also present in the ceratosaurian *Eoabelisaurus mefi*); ilium with an only ~~very~~ slightly posteriorly projecting ischiadic peduncle*; ilium without a laterally exposed ventromedial margin of the brevis fossa (only a ~~very~~ short portion of its base is exposed, also present in *Cryolophosaurus ellioti* Hammer & Hickerson, 1994); ilium with a poorly transversely expanded brevis fossa (also present in non-coelophysid neotheropods); femur with a dorsolateral trochanter on the proximal end (also present in WARMS G667–690 and non-averostran neotheropods)~~;~~ and femoral fourth trochanter ~~very~~ poorly posteriorly expanded (also present in WARMS G667–690, coelophysids~~,~~ and early ceratosaurians).

The diagnosis of the species can be expanded with the following unique combination of character states present in the referred specimens, but unknown in the holotype (autapomorphies indicated with an asterisk): femur without an anterior extensor groove on

the distal end (only known in WARMS G667–690); tibia with a fibular crest that reaches the posterior lateral hemicondyle of the proximal end; tibia with an anteroposterior depth versus mediolateral width ratio ≥ 0.6; tibia with an anteroposteriorly narrow facet for the reception of the ascending process of the astragalus (indicating a non-blocky, but rather laminar ascending process of the astragalus); tibia with an angle between the main axis of the lateral half of the facet for reception of the ascending process of the astragalus and the longitudinal axis of the bone ≥25° in anterior view; tibia with a well proximally extended posteromedial notch on the distal end; tibia with a poorly projected medial malleolus; and fibula with a poorly projected and tab-like posterior margin of the proximal end in lateral view* (only known in WARMS G667–690).

See Discussion for a differential diagnosis of the species among early neotheropods.

DESCRIPTION OF WARMS G667–690

The holotypes of *Sarcosaurus woodi* and '*Sarcosaurus andrewsi*' have been recently redescribed in detail ~~recently~~ by Carrano & Sampson (2004). Thus, we do not provide new redescriptions here, although comments on their anatomy are provided in the discussion of the taxonomy of the genus *Sarcosaurus* and we do refigure both specimens. By contrast, WARMS G667–690 was described and figured with line drawings by Huene (1932), but no detailed redescription has been provided to date.

Dorsal vertebra. A dorsal vertebra (WARMS G678) is partially preserved, including the centrum and the left lateral wall of the neural canal (Fig. 4; Table 1). The left lateral surface of the centrum is well preserved, but the anterior and posterior ends of the right lateral surface of the centrum are eroded and the lateral surface has collapsed inwards. The neurocentral suture is open (Huene, 1932) and strongly interdigitated (Fig. 4: ncs). The neural

arch preserves the distal ends of well-developed anterior and posterior centrodiapophyseal laminae, with the former lamina extending further ventrally than the latter (Fig. 4: acdl, pcdl). This element is interpreted as a middle or posterior (although not one of the most posterior) dorsal vertebra because of the degree of ventral development and primarily anteroposterior (rather than dorsoventral) orientation of the centrodiapophyseal laminae when compared to the presacral vertebral series of *Liliensternus liliensterni* (Huene, 1934) (HMN MB.R. 2175) and *Dilophosaurus wetherilli* (Welles, 1954) (UCMP 37302). The centrum is proportionally long anteroposteriorly, being c. 1.9 times longer than its anterior height, resembling the condition of the posterior dorsal vertebrae of *Eodromaeus murphi* (PVSJ 562: ratio = 2.0−2.18). This ratio is higher than in the middle–posterior dorsal vertebrae of *Liliensternus liliensterni* (HMN MB.R. 2175: highest ratio = 1.67, middle dorsal vertebra), *Dracoraptor hanigani* (NMW 2015.5G.1–2015.5G.11: ratio = 1.63−1.75, middle–posterior dorsal vertebrae), *Dilophosaurus wetherilli* (UCMP 37302: highest ratio = 1.66, dorsal 10; UCMP 77270: highest ratio = 1.73, dorsal 10), *Eoabelisaurus mefi* (MPEF PV 3990: highest ratio = 1.19, dorsal 12) and *Piatnitzkysaurus floresi* Bonaparte, 1979 (PVL 4073: ratio = 1.11, middle dorsal vertebra), but distinctly lower than in the coelophysids ~~*Procompsognathus triassicus* (SMNS 12591: 2.70−2.91, dorsals 7 and 8),~~ *Coelophysis bauri* Cope, 1887 (Melbourne specimen: ca. 2.6, middle dorsal) and *Megapnosaurus rhodesiensis* (Raath, 1969) (Raath, 1977: 2.33−2.64, dorsals 6 and 7 of QG1),~~.~~ *Procompsognathus triassicus* Fraas, 1913 (SMNS 12591: 2.70−2.91, dorsals 7 and 8). The preserved posterior dorsal vertebra of the holotype of *Sarcosaurus woodi* lacks its posterior portion, but its length:anterior height ratio as preserved is 1.00 and, thus, this ratio would have been considerably lower than 2 (NHMUK PV R4840). WARMS G678 is moderately transversely compressed around mid-length, giving it an hourglass-shape in ventral view. The ventral surface of the centrum is continuously transversely convex, without a median keel or groove. The presence of a

median ventral keel is variable along the dorsal series in early neotheropods, being, for example, present up to the sixth dorsal vertebra in the holotype of *Dilophosaurus wetherilli* (UCMP 37302). Among European early neotheropods, the available dorsal vertebrae of *Liliensternus liliensterni* (HMN MB.R. 2175) and *Dracoraptor hanigani* (NMW 2015.5G.1–2015.5G.11) and the posterior dorsal vertebra of the holotype of *Sarcosaurus woodi* (NHMUK PV R4840) also lack a ventral keel or groove. The ventral margin of the centrum of WARMS G678 is symmetrically dorsally arched in lateral view. The anterior and posterior articular surfaces of the centrum are taller than broad and slightly concave, although their original proportions are distorted by the inward collapse and erosion of the right lateral surface. The lateral surface of the centrum possesses a shallow and weakly defined fossa restricted to its dorsal half, located immediately ventral to the neurocentral suture (Huene, 1932; Fig. 4: fos). A similar fossa in the same location is present in other early neotheropods, such as *Liliensternus liliensterni* (HMN MB.R. 2175), *Dilophosaurus wetherilli* (UCMP 37302) and the holotype of *Sarcosaurus woodi* (NHMUK PV R4840).

Caudal vertebra. A second vertebra, only represented by a centrum (WARMS G679; Fig. 5; Table 1), is identified as belonging to the anterior or middle caudal series because it is proportionately lower and narrower than the middle−posterior dorsal vertebra, which is a condition that occurs in the vertebral series of the holotype of *Dilophosaurus wetherilli* (UCMP 37302). The caudal centrum lacks the dorsal half of one of its sides and the anterior and posterior articular surfaces are damaged and partially covered with sediment. The presence of a facet for articulation with the haemal arch cannot be determined because of damage to the ventral surfaces of the ends of the centrum. The centrum is similar in morphology to the centrum of the dorsal vertebra, but the anterior and posterior articular surfaces are subcircular and the lateral fossa is deeper (Fig. 5: fos). The surface for

articulation with the neural arch is complete on one side of the bone and is strongly interdigitated (Fig. 5: f.na).

Dorsal ribs. Several rib shaft fragments are preserved (WARMS G670, G675, G676, G685, G686; Fig. 6)~~,~~ and probably represent dorsal ribs. They possess a shallow groove along the shaft on what is probably the posterior surface (Fig. 6: gr). The shafts are anteroposteriorly compressed. The bone microstructure of one of these ribs (WARMS G676) is described below.

Ilium. A bone (WARMS G690) that was not described or figured by Huene (1932) is indentified here as part of the pubic peduncle of the left ilium (Fig. 7A–C; Table 2). The bone is somewhat transversely compressed taphonomically~~,~~ and its lateral and medial surfaces are slightly collapsed. The most anterior portion of a well-developed supra-acetabular crest is preserved and terminates 10 mm before the distal end of the peduncle (Fig. 7A–C: sac), as occurs in other early neotheropods [~~(~~e.g. *Dilophosaurus wetherilli*: UCMP 37302; *Liliensternus liliensterni*: HMN MB.R. 2175; *Lophostropheus airelensis* (~~:~~ Cuny & Galton, 1993); *Notatesseraeraptor frickensis*~~:~~ Zahner & Brinkmann, 2019, fig. 1j; ~~*Dilophosaurus wetherilli*: UCMP 37302]).~~ The preserved portion of the supra-acetabular crest faces mainly ventrally, resembling the condition of several early neotheropods in which the supra-acetabular crest is ventrolaterally oriented and partially obscures the acetabulum in lateral view (e.g. *Coelophysis bauri*: CM 81768; *Dilophosaurus wetherilli*: UCMP 77270; *Liliensternus liliensterni*: HMN MB.R. 2175; ~~*Procompsognathus triassicus*: SMNS 12591; *Coelophysis bauri*: CM 81768;~~ *Lophostropheus airelensis*: Cuny & Galton, 1993; *Procompsognathus triassicus*: SMNS 12591; ~~*Liliensternus liliensterni*: HMN MB.R. 2175; *Dilophosaurus wetherilli*: UCMP 77270;~~ holotype of *Sarcosaurus woodi*: NHMUK PV

R4840). The preserved portion of the acetabular roof is transversely concave and the dorsal surface of the peduncle is strongly transversely convex. The distal articular surface of the peduncle is incomplete.

Pubis. The proximal thirds of both pubes are preserved (WARMS G683/684, G688), lacking the articular surfaces for the ilium and ischium and the puboischiadic plate. The right pubis (WARMS G683/684) is slightly more proximally and distally complete (Fig. 7G–I) than the left element (WARMS G688; Fig. 7D–F; Table 2). The preserved portion of the proximal end is dorsoventrally tall in lateral view and narrows gradually towards the shaft. The anterior margin of the bone is slightly concave along the transition between the proximal end and shaft in lateral view, as occurs in *Eodromaeus murphi* (PVSJ 560, 562) and several other early neotheropods (e.g. *Coelophysis bauri*: CM 81768; *Liliensernus liliensterni*: HMN MB.R. 2175; *Notatesseraeraptor frickensis*: Zahner & Brinkmann, 2019, fig. 1i; holotype of *Sarcosaurus woodi*: NHMUK PV R4840). An oval scar, but not a tuberosity, indicates the insertion area of the M. ambiens (Carrano & Hutchinson, 2002). The lateral surface of the proximal end is gently dorsoventrally concave. The pubic apron (Fig. 7: pub.ap) arises from the posteroventral corner of the proximal end of the bone as preserved. The pubic apron twists to project increasingly more medially distally, until it is entirely medially directed. The pubic apron is restricted at the anteromedial corner of the shaft and gives this part of the bone a comma-shaped outline in cross-section. The medial edge of the pubic apron is broken in both pubes and, as a result, its transverse width cannot be determined. The lateral surface of the pubis possesses a shallow, longitudinal depression on both sides (Fig. 7: dp), resembling the condition in *Liliensternus liliensterni* (HMN MB.R. 2175) and *Megapnosaurus rhodesiensis* (cast of QG1). The pubic shafts are too incomplete to assess whether they were bowed or straight in lateral view.

Femur. Both femora are preserved (WARMS G681, G682), but are badly damaged (Figs. 8, 9; Table 2). In both cases most of the femoral head is missing, the anterior and fourth trochanters are damaged, and the distal end of the left femur only preserves part of the fibular condyle. The distal end of the left femur is strongly anteroposteriorly compressed as a result of taphonomic deformation.

The preserved portion of the head of the left femur shows that it was inturned and anteromedially oriented, as occurs in other basal dinosaurs. The anterolateral corner of the proximal end of the bone possesses a proximodistally elongated dorsolateral trochanter (= greater trochanter) (Figs. 8, 9: dltr), as occurs in most early theropods (e.g. *Eodromaeus murphi*: PVSJ 562; *Segisaurus halli*: UCMP 32101; '*Syntarsus*' *kayentakatae*: MCZ 9175, cast of MNA V2623; *Megapnosaurus rhodesiensis*: NHMUK PV R9584, cast of QG1; *Liliensternus liliensterni*: HMN MB.R. 2175; *Dilophosaurus wethherilli*: UCMP 37302; holotype of *Sarcosaurus woodi*: NHMUK PV R4840). By contrast, a distinct, proximodistally elongated dorsolateral trochanter is absent in averostrans, such as *Eoabelisaurus mefi* (MPEF PV 3990), *Ceratosaurus nasicornis* (USNM 4735) and *Piatnitzkysaurus floresi* (PVL 4073). The base of this trochanter is moderately broad in WARMS G681 and G682, but its surface is not preserved in either femur and it cannot be determined if it was sharp or mound-like. The most proximal portion of the dorsolateral trochanter is rugose and likely represents the insertion of the M. puboischiofemoralis externus (Hutchinson, 2001). The distal development of this muscle scar cannot be determined because of damage to the bone. The anterior surface of the proximal end of the femur, medial to the dorsolateral trochanter, is concave.

The base of the anterior trochanter is preserved in both femora (Figs. 8, 9: atr). The anterior trochanter has a subtriangular outline where it is broken off in the left femur,

possessing a broad base and tapering proximal end. This condition resembles that of other early theropods (e.g. *Eodromaeus murphi*: PVSJ 562; *Megapnosaurus rhodesiensis*: NHMUK PV R9584, cast of QG1; *Coelophysis bauri*: Melbourne specimen; *Liliensternus liliensterni*: HMN MB.R. 2175; *Cryolophosaurus ellioti*: Smith *et al.*, 2007; *Dilophosaurus weththerilli*: UCMP 37302; *Ceratosaurus nasicornis*: USNM 4735; holotype of *Sarcosaurus woodi*: NHMUK PV R4840), but contrasts with the aliform anterior trochanter of tetanuran theropods (e.g. *Piatnitzkysaurus floresi*: PVL 4073; *Megalosaurus bucklandii*: NHMUK PV R31806). The anterior trochanter is located adjacent to the medial margin of the shaft in anterior view. It cannot be determined whether the proximal portion of the anterior trochanter was separated from the rest of the bone by a cleft, which is the condition that occurs in the holotype of *Sarcosaurus woodi* (NHMUK PV R4840). The preserved surfaces of the anterior trochanter are finely striated and may indicate the insertion area of the M. iliotrochantericus caudalis (Hutchinson & Gatesy, 2000). Lateral to the base of the anterior trochanter there is a low, rounded, inflated area that is covered by a series of very low ridges (Figs. 8, 9: ife). This area may represent the insertion scar of the M. iliofemoralis externus and, as a result, is interpreted as homologous to the trochanteric shelf of robust morphotypes of basal neotheropods (Hutchinson, 2001), such as the holotype of *Sarcosaurus woodi* (NHMUK PV R4840). The areas of attachment of the Mm. iliotrochantericus caudalis and iliofemoralis externus are separated by a smooth and gently concave surface. There is no sharp anterior intermuscular line (which separates the origins of the Mm. femorotibialis externus and femorotibialis internus in extant crocodiles; Hutchinson, 2001) extending along the anteromedial surface of the shaft distal to the base of the anterior trochanter, contrasting with the holotype of *Sarcosaurus woodi* (NHMUK PV R4840). The absence of a trochanteric shelf and anterior intermuscular line in WARMS G681 and G682 could be a result of skeletal immaturity (Raath, Carpenter & Currie, 1990; Griffin, 2018).

The fourth trochanter is restricted to the proximal half of the bone (Figs. 8, 9: ft) and proximally extends to the level of the distal end of the anterior trochanter. The fourth trochanter is very low and blade-like, as occurs in the holotype of *Sarcosaurus woodi* (NHMUK PV R4840), coelophysids (e.g. *Megapnosaurus rhodesiensis*: NHMUK PV R9584, cast of QG1); *Segisaurus halli* Camp, 1936: UCMP 32101; '*Syntarsus*' *kayentakatae* Rowe, 1989[: MCZ 9175, cast of MNA V2623; *Megapnosaurus rhodesiensis*: NHMUK PV R9584, cast of QG1), and early ceratosaurians (e.g. *Berberosaurus liassicus* Allain *et al.*, 2007; *Ceratosaurus nasicornis*: USNM 4735; *Eoabelisaurus mefi*: MPEF PV 3990; *Berberosaurus liassicus*: Allain *et al.*, 2007). The preserved margins of the fourth trochanter on the left femur suggest that it may have been symmetric, as occurs in other neotheropods (Nesbitt, 2011). The fourth trochanter is mainly longitudinally orientated, but it slants slightly from proximomedially to distolaterally in posterior view. Immediately medial to the base of the fourth trochanter there is an oval depression that was probably associated with the insertion of the M. caudofemoralis longus (Carrano & Hutchinson, 2002) (Figs. 8, 9: cfl). A low ridge runs along the posterolateral surface of the femoral shaft from the distal end of the fourth trochanter, but does not reach the distal end of the bone. The shaft has an oval cross-section at mid-length, being slightly wider transversely than anteroposteriorly.

The distal end of the femur possesses a proximodistally well-developed mediodistal crest (Fig. 9: mdc), as occurs in other basal neotheropods (Rowe & Gauthier, 1990; Rauhut, 2003). The degree of medial development cannot be determined because the margins of the structure are broken in both femora. The preserved anterior surface of the mediodistal crest possesses a series of thin longitudinal striations that may indicate the attachment of the distal portion of the Mm. femorotibialis externus (Hutchinson, 2001) (Fig. 9: fte). The mediodistal crest does not extend as far as the distal margin of the bone and delimits a semilunate, concave depression on the medial surface of the bone. The lateral surface of the distal end of

the femur is gently anteroposteriorly convex and smooth. The cortical bone of the anterior surface of the distal end of the right femur has collapsed inwards, but the anterior margin is continuously transversely convex in distal view (Fig. 9E). As a result, an extensor fossa was absent, resembling the condition in the *Coelophysis* sp. specimen from the Chinle Formation (UCMP 129618, 'Padian's *Coelophysis*'), *Cryolophosaurus ellioti* (Smith *et al.*, 2007), *Eodromaeus murphi* (PVSJ 562), *Liliensternus liliensterni* (HMN MB.R. 2175), *Zupaysaurus rougieri* Arcucci & Coria, 2003 (PULR 076), ~~*Liliensternus liliensterni* (HMN MB.R. 2175), *Coelophysis* sp. specimen from the Chinle Formation (UCMP 129618, 'Padian's *Coelophysis*') and *Cryolophosaurus ellioti* (Smith *et al.*, 2007)~~. By contrast, an extensor fossa is present on the distal end of the femur of *Coelophysis bauri* (USNM 529376), *Dilophosaurus wetherilli* (UCMP 37302, 77270), *Megapnosaurus rhodensiensis* (NHMUK PV R9585, cast of QG CT6/G), ~~'*Syntarsus*' *kayentakatae* (MCZ 9175, cast of MNA V2623),~~ *Powellvenator podocitus* (PVL 4414-5, 8), *Segisaurus halli* (UCMP 32101), '*Syntarsus*' *kayentakatae* (MCZ 9175, cast of MNA V2623), ~~*Coelophysis bauri* (USNM 529376), *Dilophosaurus wehterilli* (UCMP 37302, 77270),~~ an indeterminate Hettangian–Sinemurian theropod from Dorset (NHMUK PV OR39496)~~,~~ and averostrans (e.g. *Ceratosaurus nasicornis*: USNM 4735; *Eoabelisaurus mefi*: MPEF PV 3990; ~~*Ceratosaurus nasicornis*: USNM 4735;~~ *Piatnitzkysaurus floresi*: PVL 4073). The presence of an extensor fossa cannot be determined in the holotype of *Sarcosaurus woodi* because of the substantial damage to and taphonomic deformation of the distal end of the bone (NHMUK PV R4840; contra Carrano & Sampson, 2004). The popliteal fossa on the posterior surface of the distal end of WARMS G682 is moderately broad and poorly extended proximally (Fig. 9: pf). Just proximal to the popliteal fossa there is a shallowly depressed and gently striated surface that probably represents the insertion of the M. adductor femoris 1 (Carrano & Hutchinson, 2002) (Fig. 9A:

af1). The infrapopliteal ridge was absent, contrasting with '*Syntarsus*' *kayentakatae* (Rowe, 1989).

The tibial condyle (= medial condyle) (Fig. 9: tc) lacks its posterior end in the right femur and is completely absent in the left one. The preserved portion of this condyle is mainly posteriorly directed in distal view and its distal surface is continuously convex. The fibular condyle (= lateral condyle) and the tibiofibular crest (Fig. 9: fc, tfc) are separated from each other by a narrow and deep groove (Fig. 9E: gr), a condition widespread among early theropods (e.g. *Dilophosaurus wetherilli*: UCMP 37302; *Eodromaeus murphi*: PVSJ 562; *Liliensternus liliensterni*: HMN MB.R. 2175; *Zupaysaurus rougieri*: PULR 076~~;~~ ~~*Dilophosaurus wetherilli*: UCMP 37302~~). Both structures form a ~~very~~ slight obtuse angle between each other on the posterolateral corner of the bone in distal view. The medial margin of the tibial condyle and the lateral margin of the fibular condyle are slightly convex in distal view. Most of the tibiofibular crest is missing and, as a consequence, it cannot be determined if it extended posteriorly beyond the level of the tibial condyle. The tibiofibular crest is placed at the level of the proximal half of the fibular condyle and extends proximally beyond this structure. Immediately proximally to the broken surface of the tibiofibular crest there is a striated surface that should represent the scar for the origin of the M. gastrocnemius pars lateralis/M. flexor hallucis longus (Carrano & Hutchinson, 2002) (Fig. 9A: gpl). The fibular condyle is more convex than the tibial one and both are separated from each other by a broad and deep intercondylar cleft in posterior view (Fig. 9A: icc). Both tibial and fibular condyles are subequally distally projected in posterior view.

Tibia. Both tibiae are preserved (WARMS G668, G680), but the cnemial crests, posterior hemicondyles of the proximal ends~~,~~ and posterolateral process of the distal ends are damaged (Figs~~.~~ 10, 11; Table 2). In addition, only the base of the fibular crest is preserved, the shaft of

the left element is strongly transversely crushed~~,~~ and the medial end of the distal end of the right element is missing. The tibia is slightly shorter than the femur and possesses a gently anteriorly bowed shaft in lateral or medial view, as is common among early neotheropods (e.g. *Liliensternus liliensterni*: HMN MB.R. 2175; *Megapnosaurus rhodensiensis*: cast of QG 1). The proximal end possesses a well anteriorly developed and slightly laterally curved cnemial crest (Figs~~.~~ 10, 11: cn), as occurs in other dinosaurs (Irmis *et al.*, 2007). The profile of the cnemial crest in medial view cannot be determined because of breakage. The very base of a diagonal, anteroproximally to posterodistally oriented elevation is present on the lateral surface of the right cnemial crest, resembling the position of the paramarginal ridges of other early neotheropods (e.g. *Dilophosaurus wetherilli*: UCMP 77270; *Liliensternus liliensterni~~s~~*: HMN MB.R. 2175; *Megapnosaurus rhodesiensis*: cast of QG1; *Powellvenator podocitus*: PVL 4414-4; ~~*Dilophosaurus wetherilli*: UCMP 77270;~~ '*Sarcosaurus andrewsi*': NHMUK PV R3542). However, although the presence of a paramarginal ridge seems likely, it should be considered tentative in this specimen because of the substantial damage present in this area.

The medial margin of the proximal end is more proximally extended than the lateral one and, as a result, the proximal surface of the bone faces proximolaterally. The posterior margins of the posterior hemicondyles are missing (Figs, 10, 11: pc) and, as a result, it cannot be determined if they were separated from each other by a groove, as in '*Sarcosaurus andrewsi*' (NHMUK PV R3542), nor can their complete posterior development be assessed. The cortical bone of the medial surface of the proximal end has collapsed in both tibiae. The medial surface of the proximal end of the right tibia is distinctly ornamented by longitudinal striations located close to the posterior margin that may represent the scar of origin of the M. gastocnemius pars medialis (Carrano & Hutchinson, 2002) (Fig. 11C: gms). The proximal half of the medial surface of the cnemial crest also possesses a similarly ornamented surface on both tibiae. Most of the lateral surface of the cnemial crest is missing in both bones.

A proximodistally well extended fibular crest is present on the centre of the lateral surface of the proximal end of the tibia (Figs. 10, 11: fc). The fibular crest reaches the posterior lateral hemicondyle of the proximal end, as occurs in other non-tetanuran neotheropods (Rauhut, 2003), including '*Sarcosaurus andrewsi*' (NHMUK PV R3542) and the indeterminate Hettangian–Sinemurian theropod from Dorset (Benson, 2010). The posterolateral surface of the proximal half of the fibular crest possesses a series of thin, parallel and longitudinally oriented striations on both tibiae (Figs. 10, 11: str). This surface may be correlated with the attachment of the interosseum tibiofibular ligament that participated in the linkage between the proximal ends of the tibia and fibula (Baumel & Witmer, 1993). The fibular crest is distally extended up to approximately the same level as the distal margin of the cnemial crest. The shaft of the tibia possesses a subtriangular cross-section, with anteromedially and laterally facing, moderately rounded apices. The anterior surface of the shaft is gently transversely convex, whereas the posterior surface is distinctly more convex.

The distal end of the bone is transversely and ~~very~~ gently posteriorly expanded with respect to the shaft. The posterior expansion is a result of the presence of a thick, longitudinal posteromedial ridge (Figs. 10, 11: pmr), a plesiomorphic condition among neotheropods (Nesbitt, 2011). This ridge separates a transversely convex posteromedial surface from a concave posterolateral surface in the distal end of the bone (Fig. 10: plc). The posterolateral surface, immediately proximal to the distal margin, possesses a series of mainly longitudinally oriented, parallel~~,~~ and thin striations (Fig. 10D: str). The posteromedial surface also possesses a series of thin, parallel longitudinal striations on an anteroposteriorly narrow, but proximodistally extended area (Fig. 10D: str). This striated surface is placed proximally to the level of the posterolateral surface in both tibiae. The medial diagonal tuberosity (sensu Ezcurra & Brusatte, 2011) that is present in *Camposaurus arizonensis*, *Megapnosaurus*

rhodensiensis and *Powellvenator podocitus* ~~and *Megapnosaurus rhodensiensis*~~ (Ezcurra & Brusatte, 2011; Ezcurra, 2017) is absent in WARMS G668, G680 and '*Sarcosaurus andrewsi*' (NHMUK PV R3542).

The anterior surface of the tibia possesses a facet for reception of the ascending process of the astragalus (Figs~~.~~ 10, 11: fap) that is proximolaterally to mediodistally oriented at an angle of 25° with respect to the horizontal plane, resembling the condition in *Cryolophosaurus ellioti* (Smith *et al.*, 2007: fig. 19b: 24º), *Dilophosaurus wetherilli* (UCMP 77270: 23º), *Eoabelisaurus mefi* (MPEF PV 3990: 24°) and *Tachiraptor admirabilis* (LPRP/USP 0747, cast of IVIC-P-2867: 23º) ~~and *Eoabelisaurus mefi* (MPEF PV 3990: 24°)~~. By contrast, this angle is lower in ~~*Zupaysaurus rougieri* (PULR 076: 19º),~~ *Liliensternus liliensterni* (HMN MB.R. 2175: ~17º), *Powellvenator podocitus* (PVL 4414-1: 18º), *Procompsognathus triassicus* (SMNS 12591: 17º), *Zupaysaurus rougieri* (PULR 076: 19º) and coelophysines (e.g. *Camposaurus arizonensis*: UCMP 34498, 10º; *Coelophysis bauri*: AMNH unnumbered, 18º; *Lepidus praecisio*: Nesbitt & Ezcurra, 2015, 15º; *Megapnosaurus rhodesiensis*: cast of QG 1, 17º). Notably, the angle between the facet for reception of the ascending process of the astragalus and the shaft is ~38° in '*Sarcosaurus andrewsi*', but this angle could be greater as preserved than was originally the case in life because of the transverse taphonomic compression that the bone has suffered. The facet for reception of the ascending process of the astragalus of WARMS G 668 and G 680 is proximodistally more developed and anteroposteriorly narrower, thus indicating the presence of a higher and more laminar ascending process of the astragalus, than in coelophysids [(~~(~~e.g. *Coelophysis bauri*: AMNH unnumbered; *Dilophosaurus wetherilli* (UCMP 77270), *Gojirasaurus quayi* (HMN MB.R. 4232.1, cast of UCM 47221), *Liliensternus liliesnterni* (HMN MB.R. 2175), *Megapnosaurus rhodesiensis*: Raath, 1977) ~~,~~ and ~~*Liliensternus liliesnterni* (HMN MB.R. 2175), *Gojirasaurus quayi* (HMN MB.R. 4232.1, cast of UCM 47221),~~ *Zupaysaurus rougieri*

(PULR 076)] ~~and *Dilophosaurus wetherilli* (UCMP 77270)~~. The degree of anteroposterior development of this facet resembles that of '*Sarcosaurus andrewsi*' (NHMUK PV R3542) and *Tachiraptor admirabilis* (LPRP/USP 0747, cast of IVIC-P-2867), but is anteroposteriorly thicker than in averostran neotheropods (e.g. *Berberosaurus liassicus*: Allain *et al.*, 2007; *Ceratosaurus nasicornis*: USNM 4735; ~~*Berberosaurus liassicus*: Allain *et al.*, 2007;~~ *Piatnitzkysaurus floresi*: MACN-Pv CH 895). Woodward (1908) recognized that the shape of the facet for the reception of the ascending process suggests closer affinities of '*Sarcosaurus andrewsi*' with Jurassic rather than Triassic theropods. This facet extends mediodistally to the preserved corner of the bone in WARMS G668, G680.

The anterior surface of the tibia immediately proximal to the facet for reception of the astragalar ascending process lacks the thick anterior diagonal tuberosity present in several coelophysoids (i.e. *Camposaurus arizonensis*, *Coelophysis bauri*, *Lepidus praecisio*, *Megapnosaurus rhodensiensis*, *Procompsognathus triassicus*~~, *Camposaurus arizonensis*, *Megapnosaurus rhodensiensis*, *Coelophysis bauri*, *Lepidus praecisio*~~; Ezcurra & Brusatte, 2011; Nesbitt & Ezcurra, 2015; Ezcurra 2017) and '*Sarcosaurus andrewsi*' (NHMUK PV R3542). By contrast, WARMS G 668 and G 680 possess in this area a series of longitudinally oriented striations, which are better preserved on the right tibia (Figs~~.~~ 10A, 11A: str). The anterior diagonal tuberosity also possesses a rough, striated surface in other neotherpoods (e.g. *Coelophysis bauri*: AMNH FARB 30615; *Procompsognathus triassicus*: SMNS 12591) and may have been involved in the attachment of homologous soft tissues. The longitudinal ridge present along the lateral surface of the distal third of the tibia of *Camposaurus arizonensis* (Ezcurra & Brusatte, 2011) is absent in WARMS G 668 and G 680 and '*Sarcosaurus andrewsi*' (NHMUK PV R3542).

The posterolateral process of the distal end is directly laterally oriented (Figs~~,~~ 10, 11: plp), but because its edge is missing in both tibiae its degree of development and complete

outline cannot be determined. There is an inflexion that separates the more distally extended posterolateral process from the medial portion of the bone, as occurs in other early neotheropods (Nesbitt & Ezcurra, 2015; Ezcurra, 2017). The medial portion of the distal end gradually expands medially with respect to the shaft in anterior or posterior view, resembling the condition in non-averostran theropods (e.g. '*Sarcosaurus andrewsi*': NHMUK PV R3542), but contrasting with the more distinct medial development present in *Tachiraptor admirabilis* (LPRP/USP 0747, cast of IVIC-P-2867) and averostrans (e.g. *Ceratosaurus nasicornis*: USNM 4735; *Eoabelisaurus mefi*: MPEF PV 3990; *Piatnitzkysaurus floresi*: MACN-Pv CH 895). The distal surface of the tibia possesses a subtriangular outline in distal view that closely resembles that present in non-averostran neotheropods (e.g. *Coelophysis bauri*: AMNH unnumbered; *Dilophosaurus wetherilli*: UCMP 77270; ~~*Zupaysaurus rougieri*: PULR 076;~~ *Liliensternus liliensterni*: HMN MB.R. 2175; ~~*Dilophosaurus wetherilli*: UCMP 77270;~~ '*Sarcosaurus andrewsi*': NHMUK PV R3542; *Zupaysaurus rougieri*: PULR 076; ~~*Coelophysis bauri*: AMNH unnumbered~~). By contrast, *Tachiraptor admirabilis* and averostrans possess a proportionally anteroposteriorly wider distal end (Rauhut, 2003; Langer *et al.*, 2014). The distal surface of the bone has a distinct posteromedial notch located immediately distal to the posteromedial ridge (Figs~~.~~ 10, 11: pmn). This notch would have received a pyramidal posteromedial process of the astragalus and is widely distributed among basal neotheropods (Ezcurra & Novas, 2007). The development of this notch is similar to that in '*Sarcosaurus andrewsi*' (NHMUK PV R3542) and some other early neotheropods (e.g. *Dilophosaurus wetherilli*: UCMP 77270; *Liliensternus liliensterni*: HMN MB.R. 2175; *Zupaysaurus rougieri*: PULR 076; ~~*Liliensternus liliensterni*: HMN MB.R. 2175; *Dilophosaurus wetherilli*: UCMP 77270~~).

Fibula. The proximal end of the left fibula (WARMS G669) is preserved (Fig. 12A–C; Table 2). This element was originally interpreted by Huene (1932) as the distal end of the left pubis, but it is too large and its morphology is not consistent with this interpretation.

The fibula is comma-shaped in proximal view, with a transversely broader anterior portion (Fig. 12C), as occurs in other early neotheropods (e.g. *Dilophosaurus wetherilli*: UCMP 37302; *Liliensternus liliensterni*: HMN MB.R. 2175; *Megapnosaurus rhodesiensis*: cast of QG1; ~~*Liliensternus liliensterni*: HMN MB.R. 2175; *Dilophosaurus wetherilli*: UCMP 37302;~~ *Piatnitzkysaurus floresi*: PVL 4073). By contrast, the anterior portion of the bone tapers in proximal view in *Eodromaeous murphi* (PVSJ 562). The proximal surface of the bone is slightly transversely convex and distinctly concave anteroposteriorly in side view, resembling the condition in several other early theropods (e.g. *Berberosaurus liassicus*: Allain *et al.*, 2007; *Dilophosaurus wetherilli*: UCMP 37302; *Dracoraptor hanigani*: NMW 2015.5G.3; *Eodromaeous murphi*: PVSJ 562; *Liliensternus liliensterni*: HMN MB.R. 2175; ~~*Dilophosaurus wetherilli*: UCMP 37302;~~ *Piatnitzkysaurus floresi*: PVL 4073~~; *Dracoraptor hangani*: NMW 2015.5G.3; *Liliensternus liliensterni*: HMN MB.R. 2175; *Berberosaurus liassicus*: Allain *et al.*, 2007~~). The posterior margin is apparently more projected than the anterior margin in lateral view, but it is difficult to determine this confidently based only on the proximal end of the bone. The posterior expansion is less conspicuous and developed than in *Coelophysis bauri* (MCZ 4331), *Dilophosaurus wetherilli* (UCMP 37302), *Dracoraptor hanigani* (NMW 2015.5G.3)~~,~~ and *Megapnosaurus rhodesiensis* (cast of QG1)~~, *Coelophysis bauri* (MCZ 4331) and *Dilophosaurus wetherilli* (UCMP 37302),~~ but resembles more closely the condition in *Eodromaeus murphi* (PVSJ 562) and *Liliensternus liliensterni* (HMN MB.R. 2175). The anterior margin of the bone is slightly weathered, but it seems to have been mostly straight. The posterior edge is straight proximally and slightly concave more distally in lateral view. The lateral surface is anteroposteriorly convex and the portion of bone

adjacent to the proximal edge is laterally inflated. This inflated surface is rounded and decreases in height posteriorly. The anterolateral surface of the bone approximately 2 cm distal to the proximal margin possesses a rugose scar, but this appears to be too proximal for the insertion of the M. iliofibularis. The medial surface of the bone is anteroposteriorly concave and lacks a ridge or well-rimmed fossa, as occurs in *Dilophosaurus wetherilli* (UCMP 37302), *Dracoraptor hanigani* (NMW 2015.5G.3) and *Liliensternus liliensterni* (HMN MB.R. 2175), ~~*Dracoraptor hanigani* (NMW 2015.5G.3) and *Dilophosaurus wetherilli* (UCMP 37302),~~ but contrasting with the presence of these features in several other early theropods (e.g. *Berberosaurus liassicus*: Allain *et al.*, 2007; *Eodromaeus murphi*: PVSJ 562; *Megapnosaurus rhodesiensis*: cast of QG1; *Powellvenator podocitus*: PVL 4414-4; *Segisaurus halli*: UCMP 32101; '*Syntarsus*' *kayentakatae*: Tykoski, 2005: fig. 93~~; *Segisaurus halli*: UCMP 32101; *Powellvenator podocitus*: PVL 4414-4; *Megapnosaurus rhodesiensis*: cast of QG1; *Berberosaurus liassicus*: Allain *et al.*, 2007~~). The most distal preserved portion of the medial surface of the bone has a depression that appears to be the result of the collapse of cortical bone.

Huene (1932) originally identified a distal end of a fibula. This bone (WARMS G674, Fig. 12D, E; Table 2) does not possess distinct characters to allow an unambiguous identification, but it is larger than would be expected and its morphology is not consistent with those of the distal half of an ulna, radius, pubis, ischium~~,~~ or metatarsal. This bone apparently lacks the anteroposterior and somewhat transverse expansion that is observed in the distal end of the fibula of other basal neotheropods (e.g. *Zupaysaurus rougieri*: PULR 076). As a result, this bone might belong to the distal portion of a fibula with a damaged distal end.

The bone possesses a straight shaft with a suboval cross-section, in which one of the shorter margins is sharper than the other. The most proximally preserved portion of the shaft

is heavily taphonomically distorted and crushed. The distal end of the bone is more compressed than the shaft and slightly anteroposteriorly expanded if interpreted as a fibula. The lateral surface of the distal end is rugose (Fig. 12E: rug), indicating a soft tissue attachment area. The medial surface of this end has a shallow, rather well-defined longitudinal groove, adjacent to which there is a rounded inflated surface (Fig. 12D: gr). There is a sharp, longitudinal ridge running along the anterior or posterior surface of the bone, which does not reach the distal margin. The distal surface is partially eroded, but its better-preserved region is ~~very~~ slightly concave.

Metatarsus. The metatarsus is represented by the distal halves of metatarsals II and IV~~,~~ and the distal portion of metatarsal III from the left side. In addition, the proximal end of a metatarsal II or III is also preserved, although it is unclear whether this element is from the left or right side (Fig. 13A–H, L; Table 2).

The preserved portion of the shaft of metatarsal II (WARMS G672) is straight and possesses a suboval cross-section, with a less convex posterolateral surface (Fig. 13A–C). The distal end of the bone is anteroposteriorly and ~~very~~ gently transversely expanded. The collateral fossae have a similar development and shape on both sides (Fig. 13A–C: clf), resembling the condition in *Liliensternus liliensterni* (HMN MB.R. 2175). By contrast, the lateral collateral fossa is distinctly bigger than the medial one in the metatarsal II of *Dilophosaurus wetherilli* (UCMP 37302) and *Megapnosaurus rhodesiensis* (cast of QG1) ~~and *Dilophosaurus wetherilli* (UCMP 37302)~~. There is no extensor fossa on the anterior surface of the bone, immediately proximal to the distal articular surface, as occurs in *Dracoraptor hanigani* (NMW 2015.10G.1a/b), *Liliensternus lilienstenri* (HMN MB.R. 2175) and *Dilophosaurus wetherilli* (UCMP 37302). There is a subtle extensor depression in the metatarsal II of *Megapnosaurus rhodesiensis* (cast of QG1). Nevertheless, there is a

subtriangular roughened area in WARMS G672 that probably is the scar of the attachment area of extensor ligaments. The distal articular surface is approximately as tall as broad (Fig. 13C). However, this surface is asymmetric in anterior and posterior views, with the lateral portion more distally developed than the medial one. As a result, the entire surface slants medially. This should have resulted in an inturned proximal phalanx, as usually occurs in the foot of other theropods (e.g. *Dilophosaurus wetherilli*: UCMP 37302). The medial and lateral halves of the distal articular surface are separated from each other by a deep median posterior groove, as it is typical of metatarsal II of neotheropods (e.g. *Dilophosaurus wetherilli*: UCMP 37302; *Liliensternus liliensterni*: HMN MB.R. 2175~~; *Dilophosaurus wetherilli*: UCMP 37302~~). The medial portion of the bone is complete and the lateral one lacks its posterior end, but as far as it is preserved it extends posteriorly up to the same level as the medial one. Therefore, the latter facet was probably more extended posteriorly than the medial one, as occurs in other neotheropods (e.g. *Dilophosaurus wetherilli*: UCMP 37302; *Liliensterni*: HMN MB.R. 2175~~); *Dilophosaurus wetherilli*: UCMP 37302)~~.

The distal portion of metatarsal III (WARMS G673) possesses a subtriangular shaft in cross-section where it is broken off (Fig. 13D–F). This is as a consequence of a gently transversely convex anterior surface and a posteriorly facing apex that forms a strongly transversely convex posterior surface. The distal end is anteroposteriorly and slightly transversely expanded with respect to the shaft. The collateral fossae are present on both sides and possess a teardrop-shaped outline, with a proximally oriented apex (Fig. 13F: clf). The medial fossa is longer and higher than the lateral one, but both possess a similar depth, as occurs in *Megapnosaurus rhodesiensis* (cast of QG1). The distal articular surface is strongly anteroposteriorly convex and rather symmetric, being slightly deeper than broad with the medial portion slightly higher than the lateral one (Fig. 13D). There is no intercondylar groove on the articular surface and only a broad and shallow notch separates both surfaces on

the posterior surface of the bone, as occurs in the metatarsal III of other neotheropods (e.g. *Dilophosaurus wetherilli*: UCMP 37302; *Lilienstenus liliensterni*: HMN MB.R. 2175~~;~~ ~~*Dilophosaurus wetherilli*: UCMP 37302~~). The anterior and posterior surfaces of the distal end are damaged, but apparently there was no extensor fossa on the former surface.

The preserved portion of shaft of metatarsal IV (WARMS G677) is straight (Fig. 13G, H), although it may have bowed laterally more proximally as is common among theropods (e.g. *Dilophosaurus wetherilli*: UCMP 37302; ~~*Megapnosaurus rhodesiensis*: cast of QG1;~~ *Liliensternus liliensterni*: HMN MB.R. 2175; *Megapnosaurus rhodesiensis*: cast of QG1~~;~~ ~~*Dilophosaurus wetherilli*: UCMP 37302~~). The distal end of the bone is severely damaged, but was transversely narrower than those of metatarsals II and III. The general shape of this distal end is consistent with that of metatarsal IV in other theropods (e.g. *Dilophosaurus wetherilli*: UCMP 37302; *Liliensternus liliensterni*: HMN MB.R. 2175; *Megapnosaurus rhodesiensis*: cast of QG1~~; *Liliensternus liliensterni*: HMN MB.R. 2175; *Dilophosaurus wetherilli*: UCMP 37302~~), but its degree of asymmetry cannot be determined. The medial surface of the distal end possesses a shallow and oval collateral fossa, with a proximodistal long axis (Fig. 13H: clf). On the lateral surface of the bone there is a ~~very~~ shallow depression that would probably have continued distally onto the lateral collateral fossa. If this was the case, then it was considerably more distally placed than that on the medial surface. This condition resembles that of *Dilophosaurus wetherilli* (UCMP 37302). The anterior surface of the distal end of the bone is missing.

The proximal end of a metatarsal is preserved (WARMS G671), but is severely damaged and most of its cortical bone is lost (Fig. 13L). The bone was apparently transversely expanded at its end and possesses a subrectangular outline in proximal view as preserved. The size and outline of the bone rule out its identification as the proximal end of metatarsals I, IV~~,~~ and V. By contrast, its size and shape are consistent with those of the

metatarsals II and III of other early neotheropods, which possesses trapezoidal and subrectangular outlines in proximal view (e.g. *Dilophosaurus wetherilli*: UCMP 37302; *Liliensternus liliensterni*: HMN MB.R. 2175~~; *Dilophosaurus wetherilli*: UCMP 37302~~). As a result, this bone is identified as either the right or left proximal end of a metatarsal II or III.

Pedal phalanx. The proximal half of a non-ungual phalanx is preserved (WARMS G687, Fig. 13I–K) and belongs to the foot because a manual phalanx would be expected to be proportionally narrower. This phalanx is large and its size fits with that expected for the most proximal phalanx of digit II or III. In addition, the outline of the bone in proximal view is identical to that of phalanx II-1 of *Dilophosaurus wetherilli* (UCMP 37302) and the height and width of the proximal end fits perfectly with the distal end of the left metatarsal II. Thus, this element is identified as a left phalanx II-1. The proximal surface is heavily covered with matrix and it cannot be determined whether the articular facet was undivided as in proximal phalanges or not. The proximal end of the bone is more expanded anteriorly than posteriorly and, as a result, the former margin of the phalanx is more arched in lateral view. The proximolateral margin is slightly more posteriorly developed than the proximomedial one and possesses a more squared corner in lateral view than the more acute medial corner. The medial margin of the proximal end has a distinct, low apex at mid-height and the lateral margin is damaged. The bone is subcircular in cross-section close to its mid-length, where it is broken off.

Dorsal rib histology. A thin section of one of the preserved rib shafts (WARMS G676) was made to examine bone microstructure (Fig. 14). This portion of the shaft is comma-shaped in cross-section, with a concave posterior and a convex anterior surface. The medial surface of the bone has broken away post-mortem and the lateral surface is strongly anteroposteriorly

convex. The shaft has a transverse width of 8.0 mm and a maximum preserved anteroposterior length of 12.4 mm. The rib thin section lacks one end and the outermost region of the bone cortex has been damaged in some areas. The subperiosteal surface underwent a prominent diagenetic alteration along nearly the entire circumference of the bone (black area on the outermost region of the slice)~~; however~~, but apart from these superficial taphonomic artefacts, the bone microstructure is otherwise ~~very~~ well-preserved. The cross-section of the rib is suboval, tapering slightly towards the missing end of the slice. There is conspicuous bone remodelling, which is particularly evident in the posterior (upper) region of the section as the compact spongy bone (Fig. 14: csb) extends close to the subperiosteal surface. Although remodelled, this tissue is not Haversian bone as it lacks cement lines. In the non-remodelled region of the slice, the primary bone is composed of fibrolamellar tissue (Fig. 14: flb), which occupies approximately 14% of the transverse width and 18% of the anteroposterior length of the section as preserved. The primary bone has a ~~very~~ high density of large, randomly organi~~z~~zed longitudinal primary osteons, which are more densely packed in the lateral (left) region of the slice. Only a few vascular canals possess circumferential anastomoses that connect to other canals. No Sharpey's fibres are present in the section. The outermost region is composed of pseudolamellar bone (= parallel-fibred bone *sensu* de Ricqlès, 1975; Fig. 14: plb) and possesses at least seven annuli visible on the upper left of the slice (Fig. 14C, D: arrowheads), with older annuli assumed to have been lost due to the underlying remodelling. The most external five annuli are closely packed, but there is some longitudinal vascularization in the zones that separate these annuli from each other and, as a result, it cannot be interpreted as an external fundamental system.

RESULTS OF THE PHYLOGENETIC ANALYSES

Analysis using *Sarcosaurus woodi*, WARMS G667–690 and '*Sarcosaurus andrewsi*' as different terminals. The analysis of the data matrix using the three neotheropod specimens from central England as different terminals found 27 most parsimonious trees (MPTs) of 1267 steps with a consistency index (CI) of 0.3631 and a retention index (RI) of 0.7052 (best score hit 73 times of the 100 replicates). The overall topology of these MPTs is mostly congruent with those recovered in the analyses of the most recent iterations of this matrix (Ezcurra, 2017; Marsola *et al.*, 2019; Marsh *et al.*, 2019b), but with some differences related to unstable terminals within Neotheropoda (see Discussion). Resembling previous analyses, we found a major dichotomy at the base of Neotheropoda between Coelophysoidea and a lineage leading to Averostra. The strict consensus tree (SCT) generated from the MPTs shows a relatively well-constrained position for the three specimens studied here. They are nested in the lineage leading to Averostra, in a polytomy together with *Tachiraptor admirabilis* and Averostra. This polytomy results from the collapse of zero-length branches because there are no synapomorphies supporting sister-taxon relationships among WARMS G667–690, '*Sarcosaurus andrewsi*' and *Sarcosaurus woodi*, or the placement of any of them closer to Averostra. The inclusion of *Tachiraptor admirabilis* in this polytomy is as a result of the placement of *Sarcosaurus woodi* as the sister-taxon of Averostra in some MPTs.

Sarcosaurus woodi is recovered as one of the most immediate sister-taxa to Averostra because of the presence of the following synapomorphies: ilium with anteroventrally oriented ventral margin of the preacetabular process in lateral view, forming a ~~very~~ narrow gap between the process and the pubic peduncle (character 376: 0->1) and femur with poorly posteriorly developed fourth trochanter, raised from the shaft as a low ridge (character 377: 0->1). WARMS G667–690 is placed in one of the successive nodes leading to Averostra because of the presence of one synapomorphy of the *Gojirasaurus quayi* + Averostra clade, tibia with angle between the main axis of the lateral half of the facet for reception of the

ascending process of the astragalus in anterior view and the longitudinal axis of the bone >20º (character 378: 1->2), and the following synapomorphies of the WARMS G667–690 + '*Sarcosaurus andrewsi*' + *Sarcosaurus woodi* + *Tachiraptor admirabilis* + Averostra clade, astragalus with plate-like/laminar ascending process (character 274: 0->1) and character state 377 (0->1, see above for its explanation). Similarly, '*Sarcosaurus andrewsi*' is recovered in the lineage leading to Averostra because of the presence of character state 274 (0->1). These two specimens are excluded from the *Tachiraptor admirabilis* + Averostra clade because of the absence of a tibia with a distinct, but shallow posteromedially opened notch on the distal end (character 343: 2->1) and with a subtriangular distal profile and an anteroposterior:mediolateral width < 0.6 (character 371: 1->2).

The Bremer supports of Neotheropoda and all less inclusive clades nested within it (with the exception of Tetanurae) are minimal (=1), whereas that of Tetanurae is 6. The absolute and GC bootstrap frequencies for Coelophysoidea, the lineage leading to Averostra and all less inclusive clades nested within it (with the exception of Averostra, Ceratosauria and Tetanurae) are lower than 50%. The resampling absolute frequency for Neotheropoda is 50% and its GC frequency is considerably lower, 33%, indicating a relatively high amount of contradictory information for this branch. Tetanurae is the best supported branch within Neotheropoda with high absolute and GC bootstrap frequencies, both of 98%. The pruning of eight topologically unstable terminals among the suboptimal trees (*Camposaurus arizonensis*, *Chindesaurus bryansmalli* Long & Murry, 1995, *Gojirasaurus quayi*, *Lepidus praecisio*, ~~*Tachiraptor admirabilis*,~~ *Lucinanovenator bonoi* Martinez & Apaldetti, 2017, ~~*Gojirasaurus quayi*,~~ *Nhandumirim waldsangae* Marsola *et al.*, 2019, ~~*Lepidus praecisio*, *Camposaurus arizonensis*, *Chindesaurus bryansmalli* and~~ *Staurikosaurus pricei* Colbert, 1970 and *Tachiraptor admirabilis*; the three specimens from central England were also recovered as unstable terminals, but they were not pruned) resulted in increased Bremer supports of 6 for

Neotheropoda, 3 for Coelophysidae and the *Panguraptor lufengensis* You *et al.*, 2014 + Coelophysinae branch, and 2 for Averostra.

Under constrained suboptimal topologies, one additional step is necessary to place *Sarcosaurus woodi* as the sister taxon of Coelophysidae (a placement supported by character state 377: 0->1) and two extra steps to find it as a ceratosaurian averostran (supported by character state 377: 0->1 in some trees and no apomorphies in other trees). WARMS G667–690 and '*Sarcosaurus andrewsi*' remain as non-averostran, non-coelophysoid neotheropods in these two constrained analyses. Regarding '*Sarcosaurus andrewsi*', one additional step is necessary to recover it as the sister-taxon of *Gojirasaurus quayi*, two extra steps are required to recover it as the earliest branching member of the lineage leading to Averostra, one of the earliest branching coelophysoids or the sister-taxon of Neotheropoda, and four extra steps for its placement as a ceratosaurian averostran (but no apomorphies support these four positions). Under these searches, *Sarcosaurus woodi* and WARMS G667–690 were found in placements close to that constrained for '*Sarcosaurus andrewsi*'. One additional step is required to find WARMS G667–690 as the sister-taxon of Coelophysidae (supported by character state 377: 0->1) and three extra steps to place it as a ceratosaurian averostran (supported by a fibula with a symmetrical or nearly symmetrical proximal portion in lateral view, character state 262: 1->0, and character state 377: 0->1).

Analysis merging *Sarcosaurus woodi*, WARMS G667–690 and '*Sarcosaurus andrewsi*' into a single terminal. The analysis of the matrix with the scoring of *Sarcosaurus woodi* (Figs. 15−17), '*Sarcosaurus andrewsi*' (Fig. 18) and WARMS G667–690 as a single terminal ('*Sarcosaurus woodi* combined') recovered nine MPTs. These trees are of 1266 steps, with a CI of 0.3633 and a RI of 0.7055 (best score hit 95 times of the 100 replicates). The MPTs show congruent topologies to those described in the previous analysis, including the

placement of '*Sarcosaurus woodi* combined' as the sister-taxon of the *Tachiraptor admirabilis* + Averostra clade (Fig. 19). The phylogenetic placement of this terminal on the branch leading to Averostra is supported by the synapomorphies of the *Gojirasaurus quayi* + Averostra clade (character state 378: 1->2), and of the '*Sarcosaurus woodi* combined' + Averostra clade (character state 274: 0->1, character state 376: 0->1). '*Sarcosaurus woodi* combined' is excluded from the *Tachiraptor admirabilis* + Averostra clade because of the absence of character states 343 (2->1) and 371 (1->2).

The Bremer supports and bootstrap frequencies are similar to those of the previous analysis, but generally slightly higher in the branches leading to Averostra. The Bremer support of the *Tachiraptor admirabilis* + Averostra branch is 2. The bootstrap absolute frequencies are of 50% or higher in the '*Sarcosaurus woodi* combined' + Averostra, and *Tachiraptor amirabilis* + Averostra branches. The pruning of topologically unstable terminals (excluding the same terminals listed for the first analysis plus *Dracoraptor hanigani* and *Liliensternus liliensterni*) from the Bremer support calculation resulted in increased values of 6 for Neotheropoda, 5 for Coelophysoidea, 4 for Averostra, 2 for the *Zupaysaurus rougieri* + Averostra and *Cryolophosaurus ellioti* + Aversotra branches, and 3 for the *Panguraptor lufengensis* + Coelophysinae branch. Tree searches using topological constrains show that two additional steps are necessary to force the position of '*Sarcosaurus woodi* combined' as the earliest branching member of the lineage leading to Averostra (no apomorphy supports this position), the sister-taxon of Neotheropoda (no apomorphy supports exclusion from Neotheropoda), or the sister-taxon of Coelophysidae (supported by character state 377: 0->1), and four extra steps to place it as a ceratosaurian averostran (supported by character states 262: 1->0 and 377: 0->1).

DISCUSSION

Ontogenetic stage of the neotheropods from the Early Jurassic of central England

The assessment of ontogenetic stage in early dinosaurs and their immediate precursors has important implications for character scorings and, thus, in the inference of the phylogenetic relationships of species (Rowe, 1989; Rowe & Gauthier, 1990; Tykoski & Rowe, 2004; Tykoski, 2005; Griffin, 2018). The bone microstructure of the rib slice of WARMS G667–690 was used to assess the ontogenetic stage of the individual at the time of its death, resembling previous studies that have used ribs to determine the degree of skeletal maturity (e.g. Erickson *et al.*, 2004). The rib thin slice of WARMS G667–690 indicates that the animal was not a juvenile because of the presence of substantial bone remodelling and several annuli, suggesting a minimum age of eight years at the time of its death. These annuli represent periods of diminution of the rate of osseous growth and there is a substantial amount of evidence that these and other growth marks (e.g. lines of arrested growth) have an annual genesis (Erickson, 2005). The number of annuli in the sampled rib should be considered as a minimum count because of bone remodelling and also because histological variation, including in the number of growth marks, is common among the bones of a single individual (Horner *et al.*, 1999, 2000). The absence of an external fundamental system indicates that the specimen had not reached somatic maturity, although its growth had probably already decelerated because of the concentration of annuli close to the periphery of the bone slice. In congruence with the histological evidence, the presence of open neurocentral sutures in the preserved dorsal and caudal vertebrae indicates skeletal immaturity because the centrum and neural arch fuses during ontogeny in both pseudosuchians and extinct dinosaurs, and in extant birds this fusion can occur before (precocial birds) or after hatching (altricial birds) (Starck, 1993; Brochu, 1996; Irmis, 2007). As a result, the absence of fusion between the tibia, fibula and proximal tarsals that is

observed in adult non-tetanuran neotheropod specimens may be a consequence of such skeletal immaturity in WARMS G667–690. In the case of the holotype of '*Sarcosaurus andrewsi*', we lack direct evidence of its ontogenetic stage. As a result, the absence of fusion between tibia, fibula and proximal tarsals cannot be unambiguously explained as a consequence of skeletal immaturity in this specimen. Beyond the ontogenetic stage, the tibia of the holotype of '*Sarcosaurus andrewsi*' is considerably longer (c. 45 cm) than that of WARMS G667–690 (c. 30 cm) (Tables 2, 3).

The holotype of *Sarcosaurus woodi* has a femoral length ~~very~~ similar to that of WARMS G667–690 (c. 32 cm; Table 4), but it shows some evidence of skeletal maturity. The ilium and pubis are fused to each other, and the femur possesses a trochanteric shelf and a distinct anterior intermuscular line, which are conditions that occur along the ontogeny of several non-tetanuran neotheropods (Rowe, 1989; Rowe & Gauthier, 1990; Tykoski & Rowe, 2004; Tykoski, 2005; Griffin & Nesbitt, 2016; Griffin, 2018). It cannot be determined if the fusion between ilium and pubis occurred in WARMS G667–690 because the articular surfaces between these bones are lost in this specimen. However, the absence of a trochanteric shelf and anterior intermuscular line suggests that WARMS G667–690 was less skeletally mature than the holotype of *Sarcosaurus woodi*, despite their similar size. The neurocentral sutures of the preserved dorsal vertebra of *Sarcosaurus woodi* appear to be closed, but poor preservation of the bone precludes a confident assessment. As a result, it can be interpreted that the holotype of *Sarcosaurus woodi* does not belong to a juvenile and was probably somewhat more skeletally mature than WARMS G667–690, but we cannot determine if it had already reached complete somatic maturity and was an adult individual at the time of its death.

Taxonomy and phylogenetic relationships of the Early Jurassic neotheropods from central England

Carrano & Sampson (2004) concluded that both *Sarcosaurus woodi* and '*Sarcosaurus andrewsi*' were *nomina dubia* because of the absence of discernable diagnostic features, and that WARMS G667–690 was referable to cf. *Sarcosaurus woodi*. The results of our phylogenetic analyses indicate that the holotypes of *Sarcosaurus woodi* and '*Sarcosaurus andrewsi*' and WARMS G667–690 possess a congruent phylogenetic signal, all three being recovered among the most immediate sister-taxa to Averostra. As a result, previous claims of a probable close relationship between these specimens (Andrews, 1921; Huene, 1932; Carrano & Sampson, 2004) are not contradicted by the evidence provided here. Another interesting result of the phylogenetic analyses is the placement of these three specimens in a part of the trees shared only with *Tachiraptor admirabilis*; in other words, there is a unique combination of apomorphies that distinguishes the English specimens from the vast majority of terminals scored in the matrix. As a consequence, these results raise the questions of whether these specimens can be actually distinguished from each other at a species level and from other neotheropod species.

The ilium of *Sarcosaurus woodi* possesses a morphology that clearly departs from those of *Liliensternus liliensterni*, coelophysids (e.g. ~~'~~*Coelophysis bauri*, *Lucianovenator bonoi* ~~*Syntarsus' kayentakatae*,~~ *Megapnosaurus rhodesiensis*, *'Syntarsus' kayentakatae*~~,~~ ~~*Coelophysis bauri, Lucianovenator bonoi*~~*i*~~) and *Cryolophosaurus ellioti* in the presence of a strongly anteroventrally oriented main axis of the preacetabular process in lateral view (unknown in *Cryolophosaurus ellioti*), an ischiadic peduncle only incipiently posteriorly projected~~,~~ and a postacetabular process with a more distinctly posteroventrally slanted dorsal margin in lateral view. Previous claims that the ilium of *Sarcosaurus woodi* closely resembles that of *Dilophosaurus wetherilli* (Carrano & Sampson, 2004) were apparently partially based

on plaster reconstructions of the ilia of the holotype of the latter species (UCMP 37302), which were figured as complete bone by Welles (1984: fig. 30a, c). Indeed, the supposed 'rounded, lobate preacetabular blade' of *Dilophosaurus wetherilli* that closely resembles the preacetabular process of *Sarcosaurus woodi* (Carrano & Sampson, 2004: 542) is fully reconstructed with plaster (Fig. 20A, B), and new specimens show that the former species has instead a more squared and horizontal preacetabular process (Tykoski, 2005: fig. 76c) that resembles the condition widespread among early neotheropods. By contrast, the ilium of *Sarcosaurus woodi* differs from that of *Dilophosaurus wetherilli* (UCMP 37302; Tykoski, 2005: fig. 76c) in the strong anteroventral orientation of the preacetabular process and the lack of a conspicuous posterior projection of the ischiadic peduncle. Instead, the partial pelvic girdle of *Sarcosaurus woodi* more closely resembles those of the ceratosaurian averostran *Ceratosaurus nasicornis*, an observation already made by Andrews (1921), and the more recently published ceratosaurian *Eoabelisaurus mefi*. Nevertheless, the species from central England differs from *Ceratosaurus nasicornis* (USNM 4735) in the absence of a ventromedial wall of the brevis fossa broadly visible in lateral view and a more pronounced inflexion between the main axes of the pre- and postacetabular processes in lateral view, and from *Eoabelisaurus mefi* (MPEF PV 3990) in the presence of a subcircular anterior articular facet in the preserved posterior dorsal vertebra (distinctly taller than broad in *Eoabelisaurus mefi*) and the absence of a well-defined iliac antitrochanter on the ischiadic peduncle (well-developed as a semilunate raised structure in *Eoabelisaurus mefi*). In addition, *Sarcosaurus woodi* also differs from these ceratosaurians, as well as other averostrans, in the presence of a dorsolateral trochanter on the proximal end of the femur and the absence of a conspicuous posterior projection of the ischiadic peduncle, which seems to be an autapomorphy of the species among early neotheropods. As a result, we consider the holotype of *Sarcosaurus*

woodi to be diagnosable using a unique combination of character states, and this genus and species are therefore taxonomically valid (contra Carrano & Sampson, 2004).

The anatomical regions that overlap between WARMS G667–690 and the holotype of *Sarcosaurus woodi* possess a congruent morphology (e.g. there are no scoring differences between both specimens in our data matrix)~~,~~ and~~,~~ as a result, we could not find evidence suggesting that these specimens belong to different species. Conversely, these two specimens can be distinguished from other early neotheropods because of the unique combination of a proportionally short middle–posterior dorsal centrum (length-anterior height ratio <2, also present in non-coelophysid theropods)~~,~~ and femur with a ~~very~~ low fourth trochanter (also present in coelophysids and early ceratosaurian averostrans) and with a dorsolateral trochanter on the proximal end (also present in non-averostran theropods). As a consequence, we consider WARMS G667–690 referable to *Sarcosaurus woodi*.

As mentioned earlier, the holotypes of *Sarcosaurus woodi* and '*Sarcosaurus andrewsi*' lack overlapping bones. However, WARMS G667–690 as a referred specimen of *Sarcosaurus woodi* provides an anatomical bridge between the holotypes. The morphology of the holotype tibia of '*Sarcosaurus andrewsi*' is mostly congruent with those of WARMS G667–690 and the main difference is the presence of a diagonal tuberosity on the anterior surface of the distal end of the bone in the former specimen. However, we consider that this difference is not enough to justify the assignment of these specimens to different species because of their ~~very~~ similar overall morphology and congruent phylogenetic signal. The tibiae of WARMS G667–690 and '*Sarcosaurus andrewsi*' differ from those of coelophysoids (here including *Liliensternus liliensterni*), *Dilophosaurus wetherilli*, *Gojirasaurus quayi*, *Zupaysaurus rougieri*~~,~~ ~~*Gojirasaurus quayi*~~ and ~~*Dilophosaurus wetherilli*~~ in the presence of an anteroposteriorly less developed facet for reception of the ascending process of the astragalus (Fig. 20C–H). On the other hand, WARMS G667–690 and '*Sarcosaurus andrewsi*' differ

from *Tachiraptor admirabilis* and Averostra in the higher ratio between the anteroposterior depth and transverse width of the distal end (>0.6) and the presence of a distinct and deep posteromedial notch that forms an indented posteromedial margin in distal view (Fig. 20G–J), and from averostrans in the absence of a well-developed medial malleolus.

In order to determine if '*Sarcosaurus andrewsi*' represents a junior synonym of *Sarcosaurus woodi*, we compare~~d~~ the former with other Early Jurassic non-coelophysoid, non-averostran theropod species. Only the partial proximal portion of a left tibia of *Dracoraptor hanigani* (early Hettangian of Wales; Martill *et al.*, 2016) can be compared with '*Sarcosaurus andrewsi*'. The comparable portion of bone has a congruent morphology in both species, but it also matches the morphology in other non-tetanuran neotheropods. As a result, we do not have enough information to distinguish the two species from each other. Nevertheless, WARMS G667–690 differs from *Dracoraptor hanigani* in the presence of a fibula with a poorly projected and tab-like posterior margin of the proximal end in lateral view. No tibia is known from the Triassic averostran-like neotheropod *Notatesseraeraptor frickensis* (latest Late Triassic of Switzerland; Zahner & Brinkmann, 2019) and only a few elements overlap with WARMS G667–690 (dorsal centrum and ribs, and partial ilium and pubis), which possess a congruent morphology. However, the phylogenetic placement of *Notatesseraeraptor frickensis* as one of the earliest branching averostran-like theropods (Zahner & Brinkmann, 2019) suggests that it is a different species ~~to~~ from WARMS G667–690 and '*Sarcosaurus andrewsi*'. The holotype of *Dracovenator regenti* Yates, 2005 (Hettangian–Sinemurian of South Africa; Yates, 2005) lacks overlapping bones with '*Sarcosaurus andrewsi*' and WARMS G667–690, whereas only part of the pubic peduncle of the ilium can be compared with the only known specimen of *Lophostropheus airelensis* (Rhaetian–Hettangian of France; Cuny & Galton, 1993; Ezcurra & Cuny, 2007). However, phylogenetic analyses suggest that these two species are not closely related to '*Sarcosaurus*

andrewsi' and WARMS G667–690 (*Dracovenator regenti* has been recovered as one of the sister-taxa to the *Dilophosaurus wetherilli* + Averostra clade, and *Lophostropheus airelensis* has been found as a coleophysoid or one of the sister-taxa to the *Dilophosaurus wetherilli* + Averostra clade; e.g. Yates, 2005; Ezcurra & Cuny, 2007; Smith *et al.*, 2007; Ezcurra, 2012; Langer *et al.*, 2014; Wang *et al.*, 2017b). The few preserved bones of the theropod *Dandakosaurus indicus* Yadagiri, 1982 (Sinemurian–Pliensbachian of India; Yadagiri, 1982; but considered a *nomen dubium* by Holtz, Molnar & Currie, 2004) do not overlap with those of '*Sarcosaurus andrewsi*' and WARMS G667–690, but the presence of opisthocoelous dorsal vertebrae (this condition suggests that they are anterior dorsal elements although Yadagiri [1982] did not specify their position in the dorsal series) suggests that it is a more derived, averostran theropod. Finally, we do not have enough information to compare the averostran-like or early averostran *Sinosaurus triassicus* Young, 1940 (Sinemurian–Pliensbachian of China; Xing *et al.*, 2014; Currie *et al.* [2019] reported in a preliminary communication that the holotype of *Shuangbaisaurus anlongbaoensis* Wang *et al.*, 2017, from the same geological unit in China, falls within the range of morphological variability of *Sinosaurus triassicus*) with the preserved bones of '*Sarcosaurus andrewsi*' and WARMS G667–690.

These comparisons show that the holotype of '*Sarcosaurus andrewsi*' and WARMS G667–690 can be distinguished from all other early neotheropod species with overlapping bones and the unique combination of character states present on the distal end of the tibia indicates that they are co-specific. As a result, we propose that the holotype of '*Sarcosaurus andrewsi*' can be referred to *Sarcosaurus woodi* and that the former species is a subjective junior synonym of the latter.

The fossil record and evolution of Early Jurassic neotheropods

The discussion of the early evolution of Neotheropoda in an explicit phylogenetic context is complicated because of the relatively unstable placement of several Late Triassic and Early Jurassic species (e.g. ~~*Liliensternus liliensterni,*~~ *Dracoraptor hanigani*, *Lepidus praecisio*, *Liliensternus liliensterni*, ~~and *Zupaysaurus rougieri,*~~ *Sarcosaurus woodi*, *Sinosaurus triassicus* and *Zupaysaurus rougieri*; Carrano, Benson & Sampson, 2012; Wang *et al.*, 2017b; Martill *et al.*, 2016; Ezcurra, 2017), even in different iterative analyses of the same phylogenetic matrix (Martill *et al.*, 2016; Ezcurra, 2017; Marsola *et al.*, 2019; Marsh *et al.*, 2019b). Here, *Lepidus praecisio* is recovered deeply nested within Coelophysidae as the sister taxon of *Coelophysis bauri*, as in Ezcurra (2017) and similar to Marsola *et al.* (2019), but contrasting with its position as the earliest member of the branch leading to Averostra in Marsh *et al.* (2019b). *Liliensternus liliensterni* is found at the base of Coelophysoidea, as occurs in Ezcurra (2017) and Marsola *et al.* (2019), but it was recovered as one of the successive sister taxa leading to Averostra in Martill *et al.* (2016) and Marsh *et al.* (2019b). *Zupaysaurus rougieri* is recovered as the earliest member of the branch leading to Averostra, resembling the results of Martill *et al.* (2016), Ezcurra (2017) and Marsh *et al.* (2019b), but Marsola *et al.* (2019) found it as a non-coelophysid coelophysoid. Finally, *Dracoraptor hanigani* is recovered here as the earliest branching coelophysoid, together with *Liliensternus liliensterni*, as ~~occurs~~ in the results of Martill *et al.* (2016), but this species was alternatively recovered in this position or within the branch leading to Averostra by Ezcurra (2017). The instability in the placement of these taxa shows that the phylogenetic relationships around the base of Neotheropoda are still in state of flux and more work is needed on this topic.

The phylogenetic position of *Sarcosaurus woodi* has been tested before in several quantitative analyses, yielding contradicting results. The first analysis was that of Rowe (1989; see also Rowe & Gauthier, 1990), which found this species as one of the earliest branching members of Ceratosauria *sensu lato* (Abelisauroidea + Coelophysoidea).

Subsequently, Ezcurra (2012) recovered *Sarcosaurus woodi* within Ceratosauria *sensu stricto* in a preliminary analysis, Wang *et al.* (2017b) found this species as one of the earliest branching averostran-likne neotheropods, and Dal Sasso, Maganuco & Cau (2018) reported it as a non-averostran neotheropod in a clade composed of *Dilophosaurus wetherilli* and *Cryolophosaurus ellioti*. Here we found *Sarcosaurus woodi* in a placement that was not previously recovered, as one of the most immediate sister-taxa to Averostra. Thus, *Sarcosaurus woodi* increases the diversity of non-coelophysoid, non-averostran neotheropods and their cosmopolitanism during the Early Jurassic, having been identified from Europe, Antarctica, North America, Africa, and probably Asia (e.g. Yates, 2005; Smith *et al.*, 2007; Dal Sasso, Maganuco & Cau, 2018). In addition, *Sarcosaurus woodi* partially fills a morphological gap between 'coelophysoid-grade' (e.g. *Zupaysaurus rougieri*, *Cryolophosaurus ellioti*, *Dilophosaurus wetherilli*, *Zupaysaurus rougieri*) and averostran theropods. For example, the femur of *Sarcosaurus woodi* possesses a dorsolateral trochanter and lacks a deep extensor fossa as in non-averostran, non-coelophysoid theropods, but it has a very low fourth trochanter as in ceratosaurian averostrans. The distal end of the tibia has a deep posteromedial notch and a relatively high distal width-depth ratio as in non-averostran neotheropods (with exception of *Tachiraptor admirabilis*), but the presence of an anteroposteriorly narrow facet for reception of the ascending process of the astragalus resembles more the condition of averostrans (Fig. 20C–J).

The oldest currently known averostran is *Saltriovenator zanellai* Dal Sasso *et al.*, 2018 from the Sinemurian of Italy (Dal Sasso, Maganuco & Cau, 2018). Nevertheless, the phylogenetic position of *Tachiraptor admirabilis* as the sister-taxon of Averostra indicates that the split between Ceratosauria and Tetanurae occurred before the Hattengian–Sinemurian boundary (ca. 199.3 Mya) (Langer *et al.*, 2014). The placement of the late Hettangian

theropod *Sarcosaurus woodi* (Fig. 21) as one of the most immediate sister-taxa to Averostra supports this inference.

ACKNOWLEDGEMENTS

We thank the following curators, researchers and collection managers that provided access to specimens under their care for the purpose of this research: Carl Mehling (AMNH), Max Langer (LPRP/USP), Daniela Schwarz (HMN), Jessica Cundiff (MCZ), Eduardo Ruigomez and Diego Pol (MPEF), Sandra Chapman and Lorna Steel (NHMUK), Caroline Buttler (NMW), Sergio Martin, Emilio Vaccari and Gabriela Cisterna (PULR), Jaime Powell, Pablo Ortíz and Rodrigo Gonzalez (PVL), Ricardo Martínez and Diego Abelín (PVSJ), Rainer Schoch (SMNS), Kevin Padian and Pat Holroyd (UCMP)~~,~~ and Michael Brett-Surman and Hans-Dieter Sues (USNM). Access to the free version of TNT 1.1 was possible due to the Willi Henning Society. Mark Witton is thanked for creating F~~f~~igures 2 and 21. This project was partially funded by a Sepkoski Grant 2019 of the Paleontological Society International Research Program (to MDE). Amy Scott-Murray (Imaging and Analysis Centre, NHMUK) carried out the scanning and produced the 3D models of NHMUK PV R4840 and R3542.

REFERENCES

Allain R, Tykoski R, Aquesbi N, Jalil NE, Monbaron M, Russell D, Taquet P. 2007. An abelisauroid (Dinosauria: Theropoda) from the Early Jurassic of the High Atlas Mountains, Morocco, and the radiation of ceratosaurs. *Journal of Vertebrate Paleontology* **27**: 610–624.

Ambrose K. 2001. The lithostratigraphy of the Blue Lias Formation (Late Rhaetian – Early Sinemurian) in the southern part of the English Midlands. *Proceedings of the Geologists' Association* **112**: 97–110.

Andrews CW. 1921. On some remains of a theropodous dinosaur from the Lower Lias of Barrow-on-Soar. *Annals and Magazine of Natural History, Series 9* **8**: 570–576.

Arcucci A, Coria RA. 2003. A new Triassic dinosaur. *Ameghiniana* **40**: 217–228.

Bakker RT. 1986. *The dDinosaur hHeresies*. Avon: Bath Press.

Baumel JJ, Witmer LM. 1993. Osteologia. In: Baumel JJ, King AS, Breazile JE, Evans HE, Vanden Berge JC, eds. *Handbook of aAvian aAnatomy: nNomina aAnatomica aAvium. 2nd eEd*. Cambridge: Nuttall Ornithology Club, 45–132.

Benson RB. 2010. The osteology of *Magnosaurus nethercombensis* (Dinosauria, Theropoda) from the Bajocian (Middle Jurassic) of the United Kingdom and a re-examination of the oldest records of tetanurans. *Journal of Systematic Palaeontology* **8**: 131–146.

Benton MJ, Martill DM, Taylor MA. 1995. The first Lower Jurassic dinosaur from Scotland: limb bone of a ceratosaur theropod from Skye. *Scottish Journal of Geology* **31**: 177–182.

Bremer K. 1988. The limits of amino acid sequence data in angiosperm phylogenetic reconstruction. *Evolution* **42**: 795–803.

Bremer K. 1994. Branch support and tree stability. *Cladistics* **10**: 295–304.

Brochu CA. 1996. Closure of neurocentral sutures during crocodilian ontogeny: implications for maturity assessment in fossil archosaurs. *Journal of Vertebrate Paleontology* **16**: 49–62.

Camp CL. 1936. A new type of small bipedal dinosaur from the Navajo Sandstone of Arizona. *University of California Publications, Bulletin of the Department of Geological Sciences* **24**: 39–56.

Carpenter K. 1997. A giant coelophysoid (Ceratosauria) theropod from the Upper Triassic of New Mexico, USA. *Neues Jahrbuch für Geologie und Paläontologie, Abhandlungen* **205**: 189–208.

Carrano MT, Hutchinson JR. 2002. Pelvic and hindlimb musculature of *Tyrannosaurus rex* (Dinosauria: Theropoda). *Journal of Morphology* **253**: 207–228.

Carrano MT, Sampson SD. 2004. A review of coelophysoids (Dinosauria: Theropoda) from the Early Jurassic of Europe, with comments on the late history of the Coelophysoidea. *Neues Jahrbuch für Geologie und Palaontologie* **9**: 537–558.

Carrano MT, Benson RB, Sampson SD. 2012. The phylogeny of Tetanurae (Dinosauria: Theropoda). *Journal of Systematic Palaeontology* **10**: 211–300.

Coddington J, Scharff N. 1994. Problems with zero-length branches. *Cladistics* **10**: 415–423.

Colbert EH. 1989. The Triassic dinosaur *Coelophysis*. *Bulletin of the Museum of Northern Arizona* **57**: 1–174.

Cope ED. 1869–1870. Synopsis of the extinct Batrachia, Reptilia and Aves of North America. *Transactions of the American Philosophical Society* **14**: 1–252.

Cope ED. 1889. On a new genus of Triassic Dinosauria. *American Naturalist* **23**: 626.

Cox BM, Sumbler MG, Ivimey-Cook HC. 1999. A formational framework for the Lower Jurassic of England and Wales (onshore area). *British Geological Survey Research Report*: **RR/99/01**: 1–28.

Cuny G, Galton PM. 1993. Revision of the Airel theropod dinosaur from the Triassic-Jurassic boundary (Normandy, France). *Neues Jahrbuch für Geologie und Paläontologie, Abhandlungen* **187**: 261–288.

Currie PJ, Xing L, Wu X, Dong Z. 2019. Anatomy and relationships of *Sinosaurus triassicus* (Theropoda, Coelophysoidea) from the Lufeng Formation (Lower Jurassic) of Yunnan, China. *Canadian Society of Vertebrate Palaeontology 2019 Abstracts*: 17.

Dal Sasso C, Maganuco S, Cau A. 2018. The oldest ceratosaurian (Dinosauria: Theropoda), from the Lower Jurassic of Italy, sheds light on the evolution of the three-fingered hand of birds. *PeerJ* **6**: e5976 .

Delsate D, Ezcurra MD. 2014. The first Early Jurassic (late Hettangian) theropod dinosaur remains from the Grand Duchy of Luxembourg. *Geologica Belgica* **17**: 175–181.

Donovan DT, Horton A, Ivimey-Cook HC. 1979. The transgression of the Lower Lias over the northern flank of the London Platform. *Journal of the Geological Society* **136**: 165−173.

Dzik J, Sulej T, Niedźwiedzki G. 2008. A dicynodont-theropod association in the latest Triassic of Poland. *Acta Palaeontologica Polonica* **53**: 733−739.

Erickson GM, Makovicky PJ, Currie PJ, Norell MA, Yerby SA, Brochu CA. 2004. Gigantism and comparative life-history parameters of tyrannosaurid dinosaurs. *Nature* **430**: 772−775.

Erickson GM. 2005. Assessing dinosaur growth patterns: a microscopic revolution. *Trends in Ecology & Evolution* **20**: 677−684.

Ezcurra MD. 2012. Phylogenetic analysis of Late Triassic – Early Jurassic neotheropod dinosaurs: implications for the early theropod radiation. *Society of Vertebrate Paleontology, Supplement to the online Journal of Vertebrate Paleontology, 2012*: 91A.

Ezcurra MD. 2017. A new early coelophysoid neotheropod from the Late Triassic of northwestern Argentina. *Ameghiniana* **54**: 506−539.

Ezcurra MD, Cuny G. 2007. The coelophysoid *Lophostropheus airelensis* nov. gen.: a review of the systematics of "*Liliensternus*" *airelensis* from the Triassic-Jurassic outcrops of Normandy (France). *Journal of Vertebrate Paleontology* **27**: 73−86.

Ezcurra MD, Novas FE. 2007. Phylogenetic relationships of the Triassic theropod *Zupaysaurus rougieri* from NW Argentina. *Historical Biology* **19**: 35−72.

Ezcurra MD, Brusatte SL. 2011. Taxonomic and phylogenetic reassessment of the early neotheropod dinosaur *Camposaurus arizonensis* from the Late Triassic of North America. *Palaeontology* **54**: 763−772.

Felsenstein J. 1985. Confidence limits on phylogenies: an approach using the bootstrap. *Evolution* **39**: 783−791.

Fraas E. 1913. Die neuestern Dinosaurierfunde der schwäbischen Trias. *Naturwissenschaften* **45**: 1097−1100.

Furin S, Preto N, Rigo M, Roghi G, Gianolla P, Crowley JL, Bowring SA. 2006. High-precision U-Pb zircon age from the Triassic of Italy: iImplications for the Triassic time scale and the Carnian origin of calcareous nannoplankton and dinosaurs. *Geology* **34**: 1009−1012.

Gauthier JA. 1986. Saurischian monophyly and the origin of birds. *Memoirs of the California Academy of Science* **8**: 1−55.

Gauthier JA, Padian K. 1985. *Phylogenetic, functional, and aerodynamic analyses of the origin of birds and their flight*. Eichstatt: The Beginning of Birds:- Freunde des Jura Museums, 185-–197.

Goloboff PA, Catalano SA. 2016. TNT version 1.5, including a full implementation of phylogenetic morphometrics. *Cladistics* **32**: 221−238.

Goloboff PA, Farris JS, Källersjö M, Oxelman B, Ramírez M, Szumik C. 2003. Improvements to resampling measures of group support. *Cladistics* **19**: 324−332.

Goloboff P, Farris J, Nixon K. 2008. TNT: a free program for phylogenetic analysis. *Cladistics* **24**: 774–786.

Griffin CT. 2018. Developmental patterns and variation among early theropods. *Journal of Anatomy* **232**: 604–640.

Griffin CT. 2019. Large neotheropods from the Upper Triassic of North America and the early evolution of large theropod body sizes. *Journal of Paleontology* **93**: 1010–1030.

Griffin CT, Nesbitt SJ. 2016. Anomalously high variation in postnatal development is ancestral for dinosaurs but lost in birds. *Proceedings of the National Academy of Sciences* **113**: 14757–14762.

Hallam A. 1997. Estimates of the amount and rate of sea-level change across the Rhaetian–Hettangian and Pliensbachian–Toarcian boundaries (latest Triassic to Early Jurassic). *Journal of the Geological Society* **154**: 773–779.

Hammer WR, Hickerson WJ. 1994. A crested theropod dinosaur from Antarctica. *Science* **264**: 828–830.

Hesselbo SP. 2008. Sequence stratigraphy and inferred relative sea-level change from the onshore British Jurassic. *Proceedings of the Geologists' Association* **119**: 19–34.

Holtz TR, Molnar R, Currie PJ. 2004. Basal Tetanurae. In: Weishampel DB, Dodson P, Osmólska H, eds. *The dDinosauria, sSecond eEdition*. Berkeley: University of California Press, 71–110.

Horner JR, de Ricqlès A, Padian K. 1999. Variation in skeletochronological indicators: implications for age assessment and physiology. *Paleobiology* **25**: 295–304.

Horner JR, de Ricqlès A, Padian K. 2000. Long bone histology of the hadrosaurid dinosaur *Maiasaura peeblesorum*: growth dynamics and physiology based on an ontogenetic series of skeletal elements. *Journal of Vertebrate Paleontology* **20**: 115–129.

Hu S. 1993. A new Theropoda (*Dilophosaurus sinensis* sp. nov.) from Yunnan, China. *Vertebrata Palasiatica* **31**: 65–69.

von Huene F ~~von~~. 1926. The carnivorous Saurischia in the Jura and Cretaceous formations, principally in Europe. *Revista del Museo de la Plata* **29**: 35–167.

von Huene F ~~von~~. 1932. Die fossile Reptil-Ordnung Saurischia, ihre Entwicklung und Geschichte. *Monographien zur Geologie und Palaeontologie, Serie* **1**: 1–361.

von Huene F ~~von~~. 1934. Ein neuer Coelurosaurier in der Thüringischen Trias. *Palaeontologische Zeitschrift* **16**: 145–170.

Hunt AP, Lucas SG, Heckert AB, Sullivan RM, Lockley MG. 1998. Late Triassic dinosaurs from the western United States. *Geobios* **31**: 511–531.

Hutchinson JR. 2001. The evolution of pelvic osteology and soft tissues on the line to extant birds (Neornithes). *Zoological Journal of the Linnean Society* **131**: 123–168.

Hutchinson JR, Gatesy SM. 2000. Adductors, abductors, and the evolution of archosaur locomotion. *Paleobiology* **26**: 734–751.

Irmis RB. 2004. First report of *Megapnosaurus* (Theropoda: Coelophysoidea) from China. *PaleoBios* **24**: 11−18.

Irmis RB. 2007. Axial skeleton ontogeny in the Parasuchia (Archosauria: Pseudosuchia) and its implications for ontogenetic determination in archosaurs. *Journal of Vertebrate Paleontology* **27**: 350−361.

Irmis RB, Nesbitt SJ, Padian K, Smith ND, Turner AH, Woody D, Downs A. 2007. A Late Triassic dinosauromorph assemblage from New Mexico and the rise of dinosaurs. *Science* **317**: 358−361.

Jaekel O. 1913. Uber die Wirbeltierfunde aus der oberen Trias von Halberstadt. *Palaeontologische Zeitschrift* **1**: 155–215.

Langer MC, Benton MJ. 2006. Early dinosaurs: aA phylogenetic study. *Journal of Systematic Palaeontology* **4**: 309–358.

Langer MC, Rincón AD, Ramezani J, Solórzano A, Rauhut OW. 2014. New dinosaur (Theropoda, stem-Averostra) from the earliest Jurassic of the La Quinta formation, Venezuelan Andes. *Royal Society Open Science* **1**: 140184.

Langer MC, Ramezani J, Da Rosa ÁA. 2018. U-Pb age constraints on dinosaur rise from south Brazil. *Gondwana Research* **57**: 133–140.

Lucas SG, Heckert AB. 2001. Theropod dinosaurs and the Early Jurassic age of the Moenave Formation, Arizona-Utah, USA. *Neues Jahrbuch für Geologie und Paläontologie-Monatshefte* **2001**: 435–448.

Marsh AD, Parker WG, Stockli DF, Martz JW. 2019a. Regional correlation of the Sonsela Member (Upper Triassic Chinle Formation) and detrital U-Pb zircon data from the Sonsela Sandstone bed near the Sonsela Buttes, northeastern Arizona, USA, support the presence of a distributive fluvial system. *Geosphere* **15**: 1128–1139.

Marsh AD, Parker WG, Langer MC, Nesbitt SJ. 2019b. Redescription of the holotype specimen of *Chindesaurus bryansmalli* Long and Murry, 1995 (Dinosauria, Theropoda), from Petrified Forest National Park, Arizona. *Journal of Vertebrate Paleontology* **39**: e1645682.

Marsh OC. 1881. Principal characters of American Jurassic dinosaurs. *American Journal of Science (3rd series)* **21**: 417–423.

Marsola JC, Bittencourt JS, Butler RJ, Da Rosa ÁA, Sayão JM, Langer MC. 2019. A new dinosaur with theropod affinities from the Late Triassic Santa Maria Formation, South Brazil. *Journal of Vertebrate Paleontology* **38**: e1531878.

Martill DM, Vidovic SU, Howells C, Nudds JR. 2016. The oldest Jurassic dinosaur: aA basal neotheropod from the Hettangian of Great Britain. *PLoS OneNE* **11**: e0145713.

Martínez RN, Apaldetti C. 2017. A late Norian-Rhaetian coelophysid neotheropod (Dinosauria, Saurischia) from the Quebrada del Barro Formation, northwestern Argentina. *Ameghiniana* **54**: 488–506.

Martínez RN, Sereno PC, Alcober OA, Colombi CE, Renne PR, Montañez IP, Currie BS. 2011. A basal dinosaur from the dawn of the dinosaur era in southwestern Pangaea. *Science* **331**: 206–210.

Munter RC, Clark JM. 2006. Theropod dinosaurs from the Early Jurassic of Huizachal Canyon, Mexico. In: Carrano MT, Gaudin TJ, Blob RW, Wible JR, eds. *Amniote paleobiology: perspectives on the evolution of mammals, birds, and reptiles*. Chicago: University of Chicago Press, 53–75.

Nesbitt SJ. 2011. The early evolution of Archosauria: relationships and the origin of major clades. *Bulletin of the American Museum of Natural History* **352**: 1−292.

Nesbitt SJ, Ezcurra MD. 2015. The early fossil record of dinosaurs in North America: aA new neotheropod from the base of the Upper Triassic Dockum Group of Texas. *Acta Palaeontologica Polonica* **60**: 513−526.

Nesbitt SJ, Smith ND, Irmis RB, Turner AH, Downs A, Norell MA. 2009. A complete skeleton of a Late Triassic saurischian and the early evolution of dinosaurs. *Science* **326**: 1530−1533.

Novas FE, Ezcurra MD, Chatterjee S, Kutty TS. 2010. New dinosaur species from the Upper Triassic Upper Maleri and Lower Dharmaram formations of central India. *Earth and Environmental Science Transactions of the Royal Society of Edinburgh* **101**: 333–349.

Old RA, Sumbler MG, Ambrose K. 1987. The geology of the country around Warwick. *Memoir of the British Geological Survey of Great Britain*, Sheet 184 (England and Wales). Keyworth: British Geological Survey.

Old RA, Hamblin RJOH., Ambrose K. 1991. The geology of the country around Redditch. *Memoir of the British Geological Survey of Great Britain*, Sheet 183 (England and Wales). Keyworth: British Geological Survey.

Owen R. 1842. Report on British fossil reptiles. Part 2. *Report of the British Association for the Advancement of Science* **11**: 60–204.

Padian K. 1986. On the type material of *Coelophysis* Cope (Saurischia: Theropoda) and a new specimen from the Petrified Forest of Arizona (Late Triassic: Chinle Formation). In: Padian K. ed. *The beginning of the age of dDinosaurs, faunal change across the Triassic-Jurassic boundary*. Cambridge: Cambridge University Press, 45–60.

Padian K, May CL. 1993. The earliest dinosaurs. The Nonmarine Triassic. *New Mexico Museum of Natural History and Science Bulletin* **3**: 379–381.

Pol D, Escapa IH. 2009. Unstable taxa in cladistic analysis: iIdentification and the assessment of relevant characters. *Cladistics* **25**: 515–527.

Pol D, Rauhut OWM. 2012. A Middle Jurassic abelisaurid from Patagonia and the early diversification of theropod dinosaurs. *Proceedings of the Royal Society B* **279**: 3170–3175.

Raath MA. 1969. A new coelurosaurian dinosaur from the Forest Sandstone of Rhodesia. *Arnoldia* **4**: 1–25.

Raath MA. 1977. *The anatomy of the Triassic theropods* Syntarsus rhodesiensis *(Saurischia: Podokesauridae) and a consideration of its biology*. Salisbury: Ph.D. thesis. Salisbury: Rhodes University., Ph.D. thesis.

Raath MA, Carpenter K, Currie PJ. 1990. Morphological variation in small theropods and its meaning in systematics: evidence from *Syntarsus*. In: Carpenter K, Currie PJ, eds. *In dDinosaur systematics: approaches and perspectives*. Cambridge: Cambridge University Press, 91–105.

Radley JD. 2003. Warwickshire's Jurassic geology, past, present and future. *Mercian Geologist* **15**: 209–218.

Ramezani J, Fastovsky DE, Bowring SA. 2014. Revised chronostratigraphy of the lower Chinle Formation strata in Arizona and New Mexico (USA): high-precision U-Pb geochronological constraints on the Late Triassic evolution of dinosaurs. *American Journal of Science* **314**: 981–1008.

Rauhut OWM, Hungerbühler A. 2000. A review of European Triassic theropods. *Gaia* **15**: 75–88.

Rauhut OWM. 2003. The interrelationships and evolution of basal theropod dinosaurs. *Special Papers in Palaeontology* **69**: 1–214.

de Ricqlès AJ ~~de~~. 1975. Recherches paleohistologiques sur les os longs des tetrapodes. VII. Sur la classification, la signification fonctionelle et l'histoire des tissues osseux des tetrapodes. Premiere partie: structures. *Annales de Paleontologie (Vertebres)* **61**: 49–129.

Rogers RR, Swisher CC, Sereno PC, Monetta AM, Forster CA, Martínez RN. 1993. The Ischigualasto tetrapod assemblage (Late Triassic, Argentina) and 40Ar/39Ar dating of dinosaur origins. *Science* **260**: 794–797.

Rowe T. 1989. A new species of the theropod dinosaur *Syntarsus* from the Early Jurassic Kayenta Formation of Arizona. *Journal of Vertebrate Paleontology* **9**: 125–136.

Rowe T, Gauthier J. 1990. Ceratosauria. In:. Weishampel DB, Dodson P, Osmólska H, eds. *The d~~D~~inosauria*. Berkeley: University of California Press, 505–518.

Sereno PC. 1998. A rationale for phylogenetic definitions, with application to the higher-level taxonomy of Dinosauria. *Neues Jahrbuch für Geologie und Paläontologie, Abhandlungen* **210**: 41–83.

Simms MJ, Chidlaw N, Morton N, Page KN. 2004. *British Lower Jurassic stratigraphy*. Peterborough: Joint Nature Conservation Committee, Geological Conservation Review Series.

Smith ND, Makovicky PJ, Hammer WR, Currie PJ. 2007. Osteology of *Cryolophosaurus ellioti* (Dinosauria: Theropoda) from the Early Jurassic of Antarctica and implications for early theropod evolution. *Zoological Journal of the Linnean Society* **151**: 377–421.

Starck JM. 1993. Evolution of avian ontogenies. *Current Ornithology* **10**: 275–366.

Swofford DL, Begle DP. 1993. *User's manual for PAUP: phylogenetic analysis using parsimony, Version 3.1*. Washington D.C.: Smithsonian Institution~~, available from authors~~.

Talbot M. 1911. *Podokesaurus holyokensis*, a new dinosaur from the Triassic of the Connecticut Valley. *American Journal of Science* **186**: 469–479.

Tykoski RS. 2005. *Osteology, ontogeny, and relationships of the coelophysoid theropods*. Ph.D. thesis. Austin: University of Texas.~~, Ph.D. thesis.~~

Tykoski RS, Rowe T. 2004. Ceratosauria. In: Weishampel DB, Dodson P, Osmólska H, eds. *The dD~~D~~inosauria, 2nd eE~~E~~dition*. Berkeley: University of California Press, 47–70.

Waldman M. 1974. Megalosaurids from the Bajocian (Middle Jurassic) of Dorset. *Palaeontology* **17**: 325–339.

Wang GF, You HL, Pan SG, Wang T. 2017a. A new crested theropod dinosaur from the Early Jurassic of Yunnan Province, China. *Vertebrata PalAsiatica* **55**: 177–186.

Wang S, Stiegler J, Amiot R, Wang X, Du GH, Clark JM, Xu X. 2017b. Extreme ontogenetic changes in a ceratosaurian theropod. *Current Biology* **27**: 144–148.

Weedon GP, Jenkyns HC, Page KN. 2017. Combined sea-level and climatic control on limestone formation, hiatuses and ammonite preservation in the Blue Lias Formation,

South Britain (uppermost Triassic – Lower Jurassic). *Geological Magazine* **155**: 1117−1149.

Welles SP. 1954. New Jurassic dinosaur from the Kayenta Formation of Arizona. *Bulletin of the Geological Society of America* **65**: 591–598.

Welles SP. 1984. *Dilophosaurus wetherilli* (Dinosauria, Theropoda) osteology and comparisons. *Palaeontographica* **185A**: 85−180.

Woodward AS. 1908. XLI.—Note on a Megalosaurian tibia from the lower Lias of Wilmcote, Warwickshire. *Annals and Magazine of Natural History* **1**: 257–259.

Xing LD, Paulina-Carabajal A, Currie PJ, Xu X, Zhang J, Wang T, Burns ME, Dong Z. 2014. Braincase anatomy of the basal theropod *Sinosaurus* from the Early Jurassic of China. *Acta Geologica Sinica* **88**: 1653–1664.

Yadagiri P. 1982. *Osteological studies of a carnosaurian dinosaur from Lower Jurassic Kota Formation: Andhra Pradesh. Geological Survey of India*. Progress Report for Field Season Programme 1981–1982, 2–7.

Yates AM. 2005. A new theropod dinosaur from the Early Jurassic of South Africa and its implication for the early evolution of theropods. *Palaeontologia Africana* **41**: 105−122.

You H-L, Azuma Y, Wang T, Wang Y-M, Dong Z-M. 2014. The first well-preserved coelophysoid theropod dinosaur from Asia. *Zootaxa* **3873**: 233–249.

Young CC. 1948. On two new Saurischia from Lufeng, Yunnan. *Bulletin of the Geological Society of China* **28(1–2)**: 75–90.

Zahner M, Brinkmann W. 2019. A Triassic averostran-line theropod from Switzerland and the early evolution of dinosaurs. *Nature Ecology & Evolution* **3**: 1146−1152.

FIGURE LEGENDS

Figure 1. Map showing the geographic occurrences of the holotype of *Sarcosaurus woodi* (Barrow-on-Soar) and referred specimens (Wilmcote) indicated with stars. The outcrop of the Lias Group is shown in grey.

Figure 2. Silhouette showing the preserved bones of referred specimen of *Sarcosaurus woodi*, WARMS G667–690. Skeletal reconstruction from Mark Witton.

Figure 3. Close-up of bioencrusters on the anterior surface of the left femur of referred specimen of *Sarcosaurus woodi* (WARMS G681).

Figure 4. Middle or posterior dorsal vertebra of referred specimen of *Sarcosaurus woodi*, WARMS G678, in left lateral (A), right lateral (B), ventral (C) and anterior (D) views. Arrows point towards anterior direction. Abbreviations: acdl, anterior centrodiapophyseal lamina; fos, fossa on lateral surface of centrum; ncs, neurocentral suture; pcdl, posterior centrodiapophyseal lamina.

Figure 5. Anterior or middle caudal vertebra of referred specimen of *Sarcosaurus woodi*, WARMS G679, in ventral (A), dorsal (B) and lateral (C, D) views. Abbreviations: f.na, interdigitated articular facet for neural arch; fos, fossa on lateral surface of centrum.

Figure 6. Fragmentary dorsal rib shafts of referred specimen of *Sarcosaurus woodi*, WARMS G670 (A, B), G675 (C, D) and G676 (E) in probable posterior (A, E) and anterior (B, C, D) views. Abbreviation: gr, groove.

Figure 7. Pelvic fragments of referred specimen of *Sarcosaurus woodi*, WARMS G690 (A–C), G688 (D–F) and G683/G684 (G–I). Partial pubic peduncle of left ilium in posterior (A) and lateral (B) views, and cross section of peduncle (C). Partial left pubis in lateral (D), medial (E) and anterodorsal (F) views. Partial right pubis in lateral (G), medial (H) and anterodorsal (I) views. Arrows point towards anterior direction. Abbreviations: dp, longitudinal depression; pub.ap, pubic apron; sac, supraacetabular crest.

Figure 8. Left femur of referred specimen of *Sarcosaurus woodi*, WARMS G681, in posterior (A), medial (B), anterior (C) and lateral (D) views. Arrows point towards anterior direction. Abbreviations: atr, anterior trochanter; cfl, depression associated with the insertion of the *M. caudofemoralis longus*; dltr, dorsolateral trochanter; ft, fourth trochanter; ife, insertion scar of the *M. iliofemoralis externus*; ri, ridge.

Figure 9. Right femur of referred specimen of *Sarcosaurus woodi*, WARMS G682, in posterior (A), medial (B), anterior (C), lateral (D) and distal (E) views. Arrows point towards anterior direction. Abbreviations: af1, insertion of the *M. adductor femoris 1*; atr, anterior trochanter; cfl, depression associated with the insertion of the *M. caudofemoralis longus*; dltr, dorsolateral trochanter; fc, fibular condyle; ft, fourth trochanter; fte, attachment of the distal portion of the *M. femorotibialis externus*; gpl, insertion scar of the *M. gastrocnemius pars lateralis/M. flexor hallucis longus*; gr, groove; icc, intercondylar cleft; ife, insertion scar of the *M. iliofemoralis externus*; mdc, mediodistal crest; pf, popliteal fossa; tc, tibial condyle; tfc, tibiofibular crest.

Figure 10. Left tibia of referred specimen of *Sarcosaurus woodi*, WARMS G668, in anterior (A), lateral (B), medial (C), posterior (D), proximal (E) and distal (F) views. Arrows point

towards anterior direction. Abbreviations: cn, cnemial crest; fap, facet for reception of ascending process of astragalus; fc, fibular crest; pc, posterior hemicondyles; plc, posterolateral concavity; plp, posterolateral process; pmn, posteromedial notch; pmr, posteromedial ridge; str, striations.

Figure 11. Right tibia of referred specimen of *Sarcosaurus woodi*, WARMS G680, in anterior (A), lateral (B), medial (C), posterior (D), proximal (E) and distal (F) views. Arrows point towards anterior direction. Abbreviations: cn, cnemial crest; fap, facet for reception of ascending process of astragalus; fc, fibular crest; gms, origin scar of the M. *gastocnemius pars medialis*; pc, posterior hemicondyles; plp, posterolateral process; pmn, posteromedial notch; pmr, posteromedial ridge; str, striations.

Figure 12. Fibula of referred specimen of *Sarcosaurus woodi*, WARMS G669 (A−C) and G674 (D, E). Proximal end of left fibula in lateral (A), medial (B) and proximal (C) views. Distal portion of fibula from indeterminate side in lateral/medial views (D, E). Arrows point towards anterior direction. Abbreviations: gr, groove; rug, rugosity.

Figure 13. Partial left pedal autopodium (A−K) and metatarsal of indeterminate side (L) of referred specimen of *Sarcosaurus woodi*, WARMS G672 (A−C), G673 (D−F), G677 (G, H), G687 (I−K) and G671 (L). Metatarsal II in anterior (A), lateral (B) and distal (C) views. Metatarsal III in proximal (D), anterior (E) and lateral (F) views. Metatarsal IV in anterior (G) and lateral (H) views. Phalanx II-1 in anterior (I), proximal (J) and lateral (K) views. Proximal end of metatarsal II or III in lateral/medial view (L). Arrows point towards anterior direction. Abbreviations: clf, collateral fossa.

Figure 14. Photomicrographs of a thin section of dorsal rib shaft of referred specimen of *Sarcosaurus woodi*, WARMS G676, under plain-polarized light (A, C) and polarized light with a gypsum plate (B, D). White rectangles in (A, B) indicate the magnified areas shown in (C, D). Arrowheads in (C, D) indicate annuli. Abbreviations: csb, compact spongy bone; flb, fibrolamellar bone; plb, pseudolamellar bone; trb, trabeculae.

Figure 15. Posterior dorsal vertebra of holotype of *Sarcosaurus woodi*, NHMUK PV R4840, in left lateral (A), right lateral (B), ventral (C), dorsal (D), anterior (E) and posterior (F) views. Arrows point towards anterior direction. Abbreviations: aaf, anterior articular facet; hyp, hypantrum; lfo, lateral fossa; prz, prezygapophysis; tp, transverse process.

Figure 16. Partial pelvic girdle of holotype of *Sarcosaurus woodi*, NHMUK PV R4840. Photographs (A−D) and surface scans (E, F) of left ilium and pubis (A, B) and right ilium and pubis (C−F) in lateral (A, C), medial (B, D), lateral and slightly posterior (E), and dorsal and slightly lateral (F) views. Arrows point towards anterior direction. Grey shaded regions are reconstructed. Abbreviations: brs, brevis shelf; brs-sac connection between brevis shelf and supraacetabular crest; isp, ischiadic peduncle; obt, obturator foramen; pipl, puboischiadic plate; pla, plaster; poap, postacetabular process; prap, preacetabular process; pub, pubis; pup, pubic peduncle; sac, supraacetabular crest.

Figure 17. Left femur of holotype of *Sarcosaurus woodi*, NHMUK PV R4840. Photographs (A−D) and surface scan (E) in posterior (A), medial (B), anterior (C), lateral (D), and lateral and slightly anterior (E) views. Arrows point towards anterior direction. Abbreviations: aiml, anterior intermuscular line; atr, anterior trochanter; cfl, depression associated with the

insertion of the *M. caudofemoralis longus*; dltr, dorsolateral trochanter; ft, fourth trochanter; trsh, trochanteric shelf.

Figure 18. Right tibia of referred specimen of *Sarcosaurus woodi*, NHMUK PV R3542 (holotype of '*Sarcosaurus andrewsi*'). Photographs (A−F) and surface scan (G) in lateral (A), medial (B), anterior (C), posterior (D), proximal (E), distal (F), and medial and slightly anterior (G) views. Arrows point towards anterior direction. Abbreviations: adt, anterior diagonal tuberosity; cn, cnemial crest; fap, facet for reception of ascending process of astragalus; fc, fibular crest; mma, medial malleolus; pamr, paramarginal ridge; pc, posterior hemicondyles; plp, posterolateral process; pmn, posteromedial notch; pmr, posteromedial ridge.

Figure 19. Time-calibrated strict consensus tree showing the phylogenetic relationships of selected non-neotheropod and all neotheropod species sampled in the phylogenetic analysis. Values next to each branch represent Bremer support, absolute bootstrap frequency, and GC bootstrap frequency, respectively. Thick black bars with a vertical line represent the chronostratigraphic uncertainty of taxa and thick black bars without a vertical line represent biochrons.

Figure 20. Comparison among partial ilia in lateral view (A, B) and tibiae in distal view (C−J) of selected neotheropod species. *Dilophosaurus wetherilli* (A, F), *Sarcosaurus woodi* (B, G, H), *Coelophysis bauri* (C), *Liliensternus liliensterni* (D), *Zupaysaurus rougieri* (E), *Tachiraptor admirabilis* (I) and *Piatnitzkysaurus floresi* (J). UCMP 37302 (A), NHMUK PV R4840 (B), AMNH unnumbered, reversed (C), HMN MB.R. 2175 (D), PULR 076 (E), UCMP 77270 (F), composite reconstruction using WARMS G668, 680 (G), NHMUK PV

R3542 (H), LPRP/USP 0747, cast of IVIC-P-2867 (I) and MACN-Pv CH 895, reversed (J). Arrows point towards anterior direction. Abbreviations: fap, facet for reception of ascending process of astragalus; isp, ischiadic peduncle; pla, plaster; plp, posterolateral process; pmr, posteromedial ridge; pmn, posteromedial notch; poap, postacetabular process; prap, preacetabular process; pub, pubis; vmbf, ventromedial margin of brevis fossa. (C−J) Not to scale.

Figure 21. Life reconstruction of the non-averostran neotheropod *Sarcosaurus woodi* from the late Hettangian−early Sinemurian of central England. Artwork by Mark Witton, who retains the copyright.

TABLES

Table 1. Measurements (in millimetres) of the preserved vertebrae of WARMS G667–690, referred specimen of *Sarcosaurus woodi*. Values in parentheses indicate incomplete measurements (owing to post-mortem damage), values in square brackets indicate estimated measurements (owing to post-mortem deformation) and the value given is the maximum measurable. The maximal deviation of the calliper is 0.02 mm, but measurements were rounded to the nearest 0.1 mm. Abbreviations: a-m C, anterior-middle caudal vertebra; m-p D, middle-posterior dorsal vertebra.

	m-p D	*a-m C*
Centrum length	44.3	50.3
Centrum anterior height	[26.5]	-
Centrum anterior width	[21.0]	-
Centrum posterior height	[27.0]	-
Centrum posterior width	[22.4]	-
Centrum height	-	21.3
Centrum width	-	19.3
Vertebra height	(44.7)	(26.3)

Table 2. Measurements (in millimetres) of pelvic and hindlimb bones of WARMS G667–690, referred specimen of *Sarcosaurus woodi*. Values in parentheses indicate incomplete measurements (owing to post-mortem damage), values in square brackets indicate estimated measurements (owing to post-mortem deformation) and the value given is the maximum measurable. The maximal deviation of the calliper is 0.02 mm, but measurements were rounded to the nearest 0.1 mm. Abbreviations: Dist, distal; Pr, proximal.

	Length	*Pr depth*	*Pr width*	*Dist depth*	*Dist width*
Iliac pubic peduncle	(45.3)	-	-	(28.3)	(16.9)
Pubis (right)	(107.2)	(34.3)	(11.7)	-	-
Pubis (right)	(84.4)	(16.9)	-	-	-
Femur (right)	(286)	-	-	(35.0)	(50.9)
Femur (left)	[317]	(40.8)	(19.9)	(26.9)	-
Tibia (right)	(296)	(55.6)	(21.8)	26.1	(32.9)
Tibia (left)	[297]	(53.8)	[24.8]	(25.0)	(33.4)
Fibula proximal end (left)	(45.9)	37.8	13.6	-	-
Fibula distal portion	(114.7)	-	-	20.3	11.8
Metatarsal II (left)	(94.8)	-	-	(18.3)	(17.2)
Metatarsal III (left)	(42.1)	-	-	(18.7)	17.8
Metatarsal IV (left)	(80.1)	-	-	(16.7)	(14.0)

Table 3. Measurements (in millimetres) of referred specimen of *Sarcosaurus woodi* (right tibia, NHMUK PV R4840, holotype of '*Sarcosaurus andrewsi*'). Values in parentheses indicate incomplete measurements (owing to post-mortem damage), values in square brackets indicate estimated measurements (owing to post-mortem deformation) and the value given is the maximum measurable. The maximal deviation of the calliper is 0.02 mm, but measurements were rounded to the nearest 0.1 mm.

Length	450
Proximal depth	104.6
Proximal width	[43.0]
Distal depth	41.7
Distal width	64.4

Table 4. Selected measurements (in millimetres) of preserved bones of the holotype of *Sarcosaurus woodi* (NHMUK PV R4840). Values in parentheses indicate incomplete measurements (owing to post-mortem damage), values in square brackets indicate estimated measurements (owing to post-mortem deformation) and the value given is the maximum measurable. The maximal deviation of the calliper is 0.02 mm, but measurements were rounded to the nearest 0.1 mm.

Centrum length	(39.8)
Centrum anterior height	39.6
Centrum anterior width	(36.5)
Femoral length (left)	(316)

SUPPORTING INFORMATION

Additional Supporting Information may be found in the online version of this article at the publisher's website:

Supporting Information I. Modifications to the phylogenetic character matrix of Nesbitt *et al*. (2009) and its subsequent iterations.

Supporting Information II. Phylogenetic data matrix in NEXUS format.

Supporting Information III. Phylogenetic data matrix in TNT format.

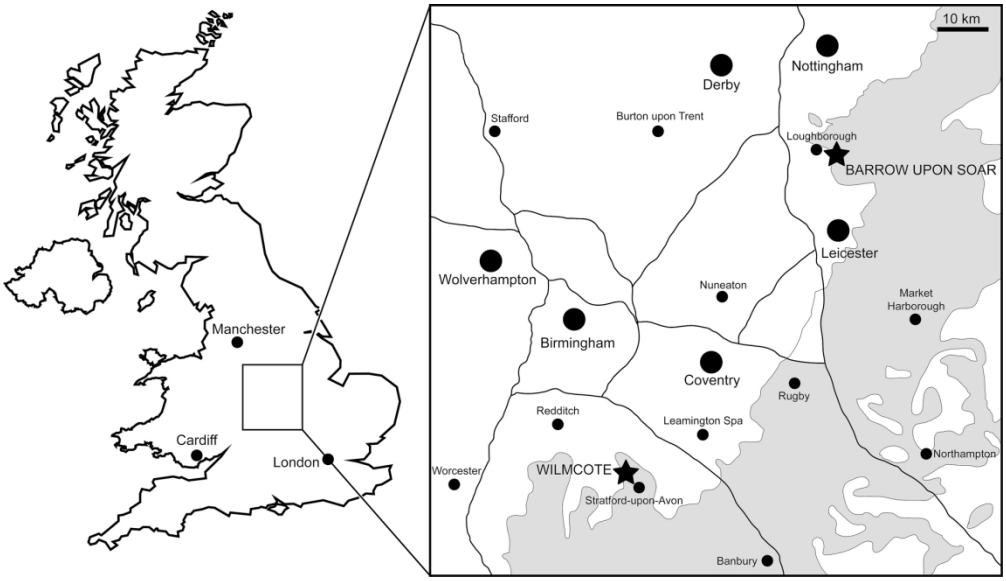

Figure 1. Map showing the geographic occurrences of the holotype of Sarcosaurus woodi (Barrow-on-Soar) and referred specimens (Wilmcote) indicated with stars. The outcrop of the Lias Group is shown in grey.

167x96mm (300 x 300 DPI)

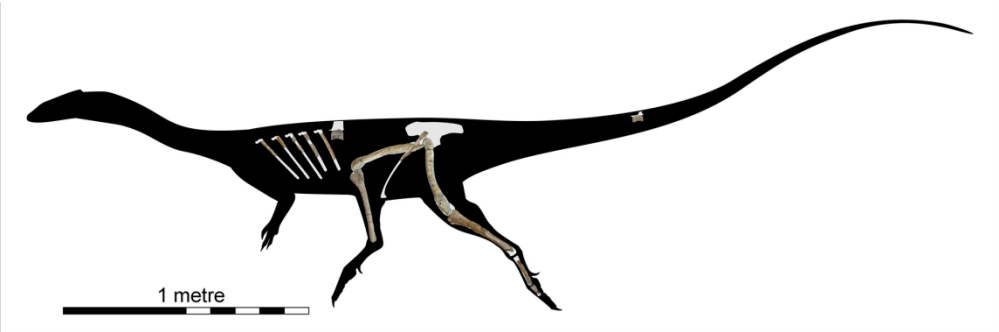

Figure 2. Silhouette showing the preserved bones of referred specimen of Sarcosaurus woodi, WARMS G667–690. Skeletal reconstruction from Mark Witton.

167x55mm (300 x 300 DPI)

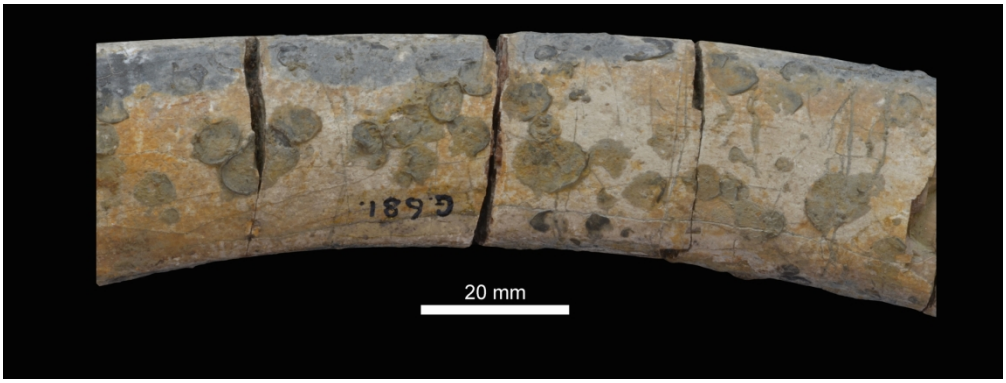

Figure 3. Close-up of bioencrusters on the anterior surface of the left femur of referred specimen of Sarcosaurus woodi (WARMS G681).

167x62mm (300 x 300 DPI)

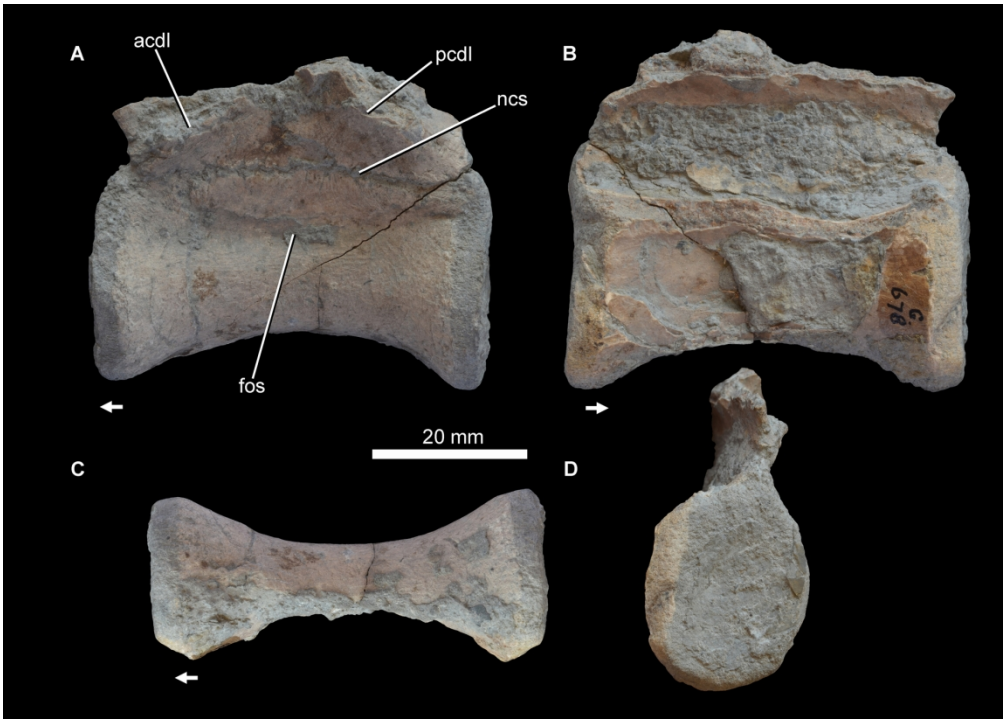

Figure 4. Middle or posterior dorsal vertebra of referred specimen of Sarcosaurus woodi, WARMS G678, in left lateral (A), right lateral (B), ventral (C) and anterior (D) views. Arrows point towards anterior direction. Abbreviations: acdl, anterior centrodiapophyseal lamina; fos, fossa on lateral surface of centrum; ncs, neurocentral suture; pcdl, posterior centrodiapophyseal lamina.

167x119mm (300 x 300 DPI)

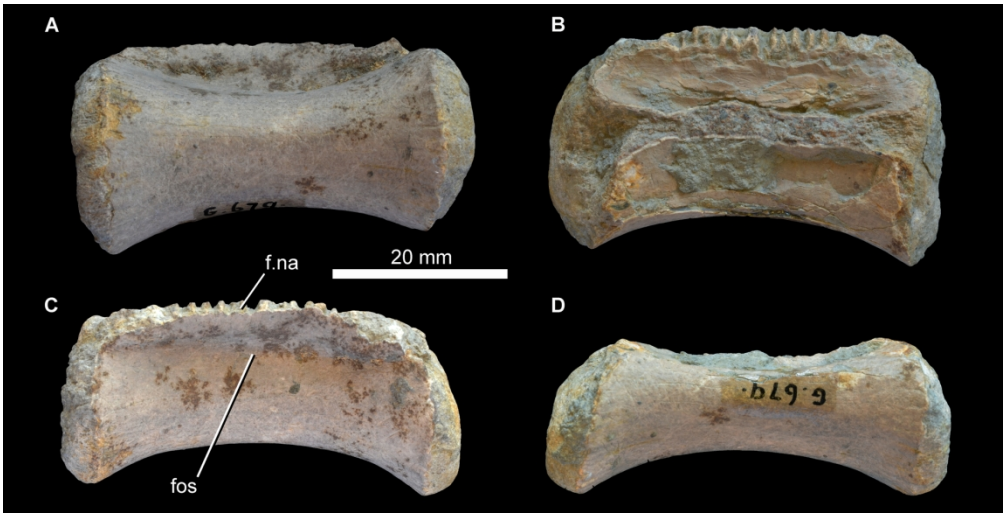

Figure 5. Anterior or middle caudal vertebra of referred specimen of Sarcosaurus woodi, WARMS G679, in ventral (A), dorsal (B) and lateral (C, D) views. Abbreviations: f.na, interdigitated articular facet for neural arch; fos, fossa on lateral surface of centrum.

167x85mm (300 x 300 DPI)

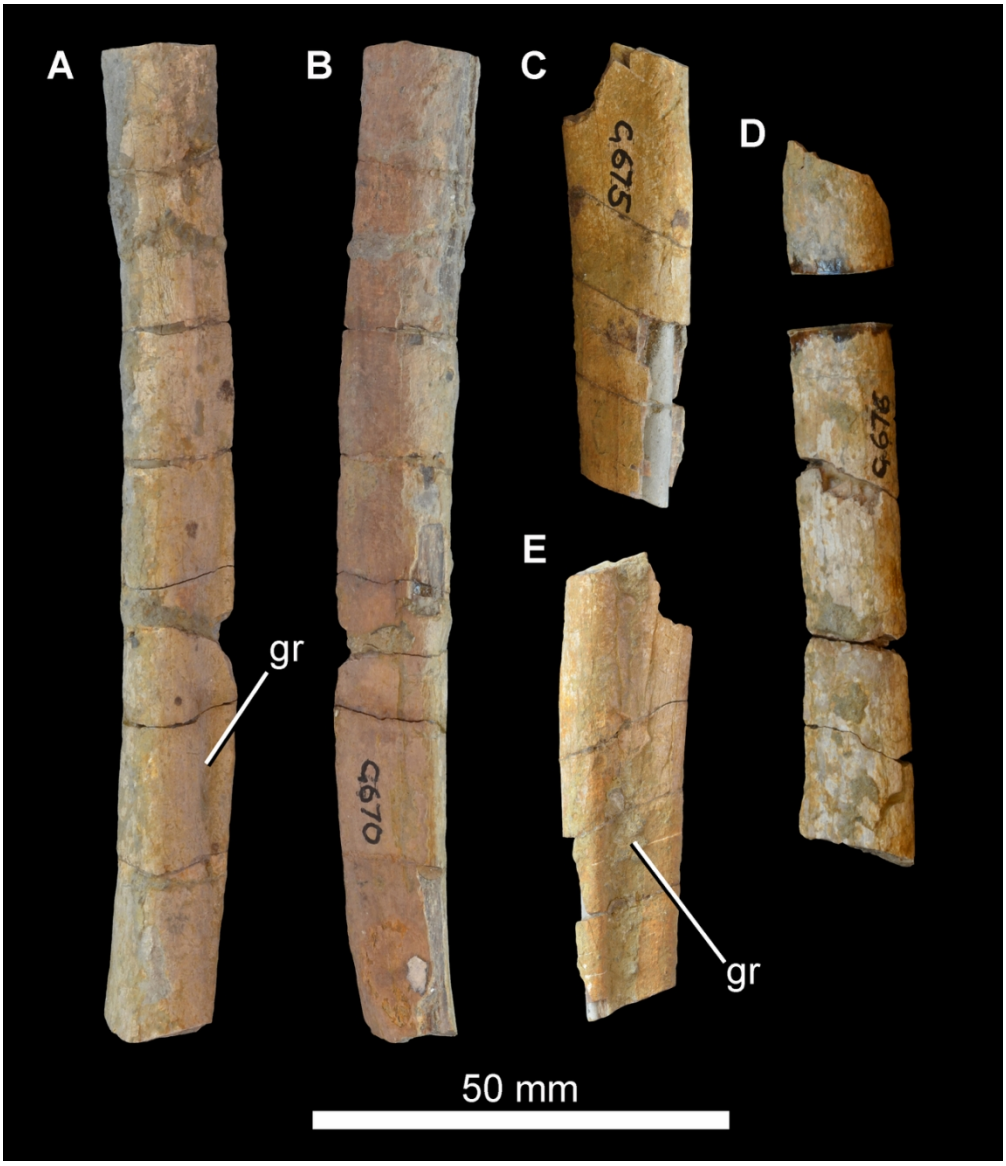

Figure 6. Fragmentary dorsal rib shafts of referred specimen of Sarcosaurus woodi, WARMS G670 (A, B), G675 (C, D) and G676 (E) in probable posterior (A, E) and anterior (B, C, D) views. Abbreviation: gr, groove.

109x126mm (300 x 300 DPI)

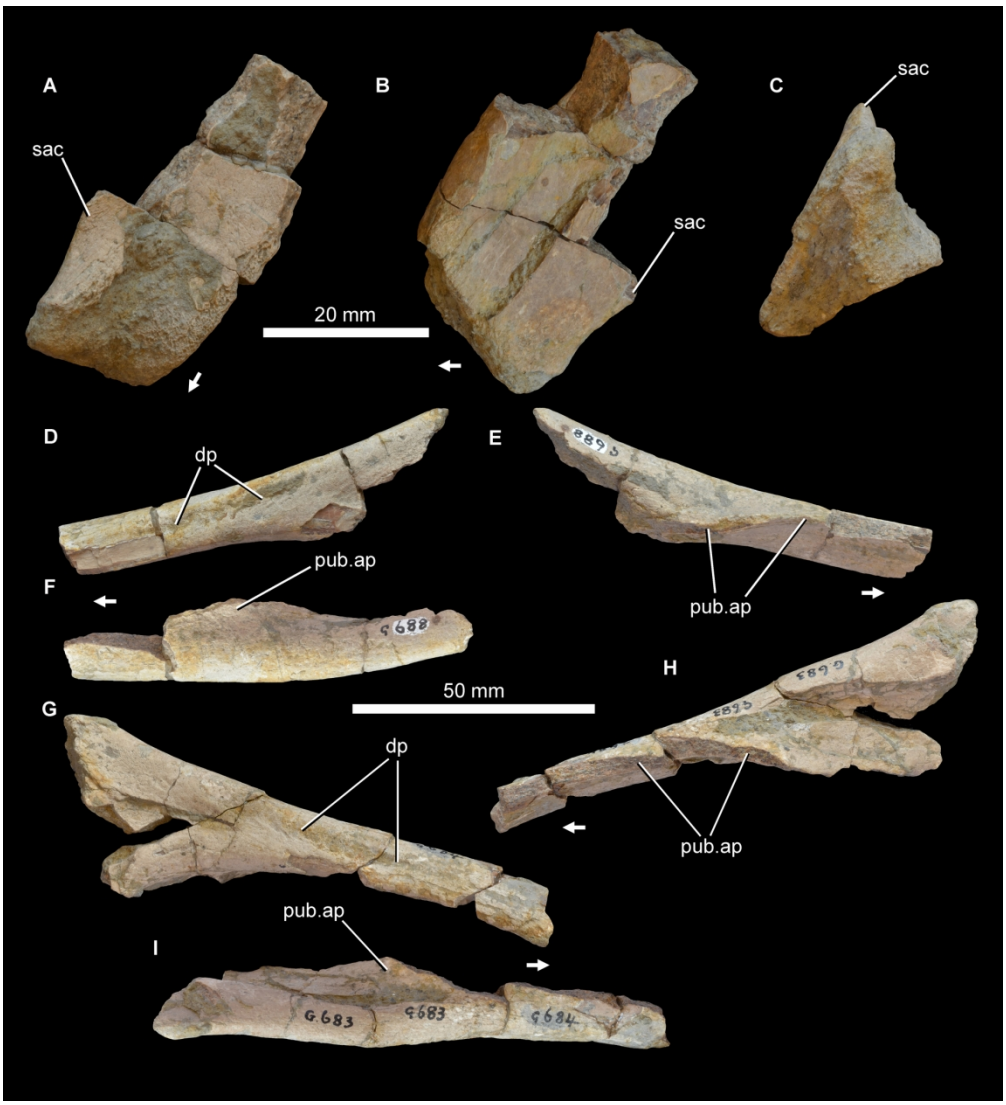

Figure 7. Pelvic fragments of referred specimen of Sarcosaurus woodi, WARMS G690 (A–C), G688 (D–F) and G683/G684 (G–I). Partial pubic peduncle of left ilium in posterior (A) and lateral (B) views, and cross section of peduncle (C). Partial left pubis in lateral (D), medial (E) and anterodorsal (F) views. Partial right pubis in lateral (G), medial (H) and anterodorsal (I) views. Arrows point towards anterior direction. Abbreviations: dp, longitudinal depression; pub.ap, pubic apron; sac, supraacetabular crest.

167x183mm (300 x 300 DPI)

Figure 8. Left femur of referred specimen of Sarcosaurus woodi, WARMS G681, in posterior (A), medial (B), anterior (C) and lateral (D) views. Arrows point towards anterior direction. Abbreviations: atr, anterior trochanter; cfl, depression associated with the insertion of the M. caudofemoralis longus; dltr, dorsolateral trochanter; ft, fourth trochanter; ife, insertion scar of the M. iliofemoralis externus; ri, ridge.

167x165mm (300 x 300 DPI)

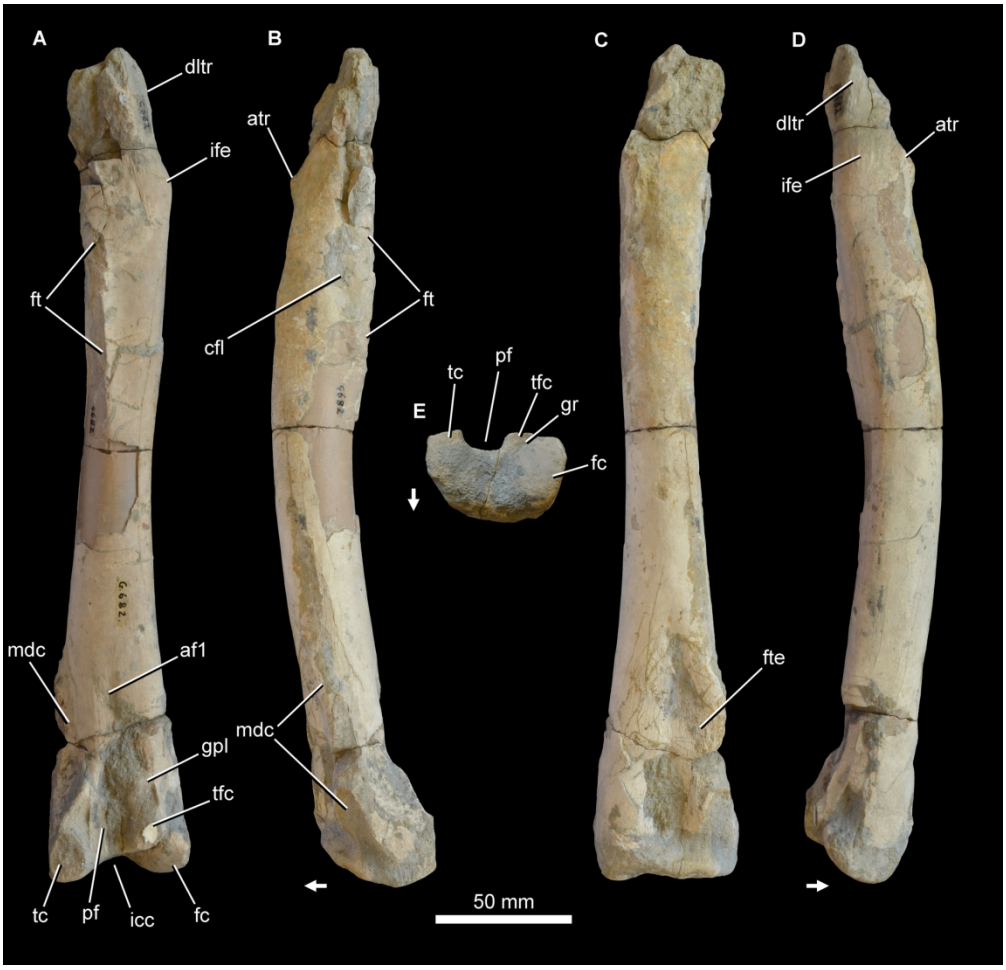

Figure 9. Right femur of referred specimen of Sarcosaurus woodi, WARMS G682, in posterior (A), medial (B), anterior (C), lateral (D) and distal (E) views. Arrows point towards anterior direction. Abbreviations: af1, insertion of the M. adductor femoris 1; atr, anterior trochanter; cfl, depression associated with the insertion of the M. caudofemoralis longus; dltr, dorsolateral trochanter; fc, fibular condyle; ft, fourth trochanter; fte, attachment of the distal portion of the M. femorotibialis externus; gpl, insertion scar of the M. gastrocnemius pars lateralis/M. flexor hallucis longus; gr, groove; icc, intercondylar cleft; ife, insertion scar of the M. iliofemoralis externus; mdc, mediodistal crest; pf, popliteal fossa; tc, tibial condyle; tfc, tibiofibular crest.

167x161mm (300 x 300 DPI)

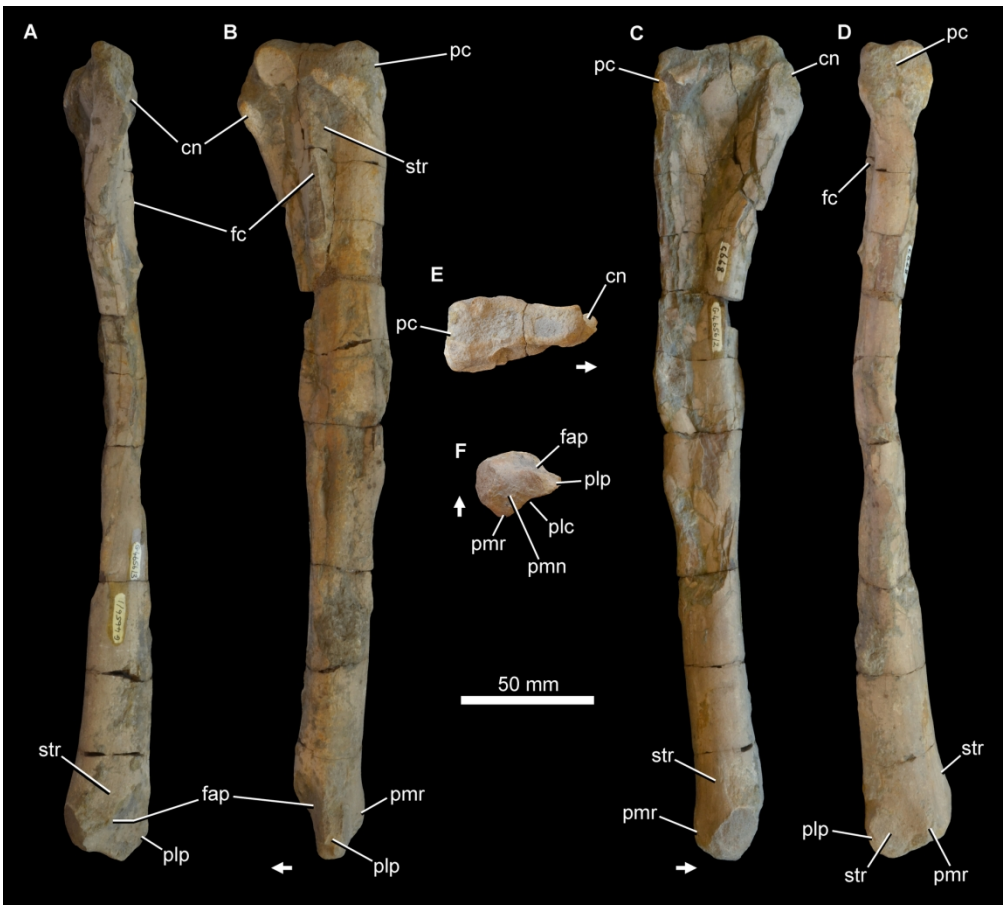

Figure 10. Left tibia of referred specimen of Sarcosaurus woodi, WARMS G668, in anterior (A), lateral (B), medial (C), posterior (D), proximal (E) and distal (F) views. Arrows point towards anterior direction. Abbreviations: cn, cnemial crest; fap, facet for reception of ascending process of astragalus; fc, fibular crest; pc, posterior hemicondyles; plc, posterolateral concavity; plp, posterolateral process; pmn, posteromedial notch; pmr, posteromedial ridge; str, striations.

167x151mm (300 x 300 DPI)

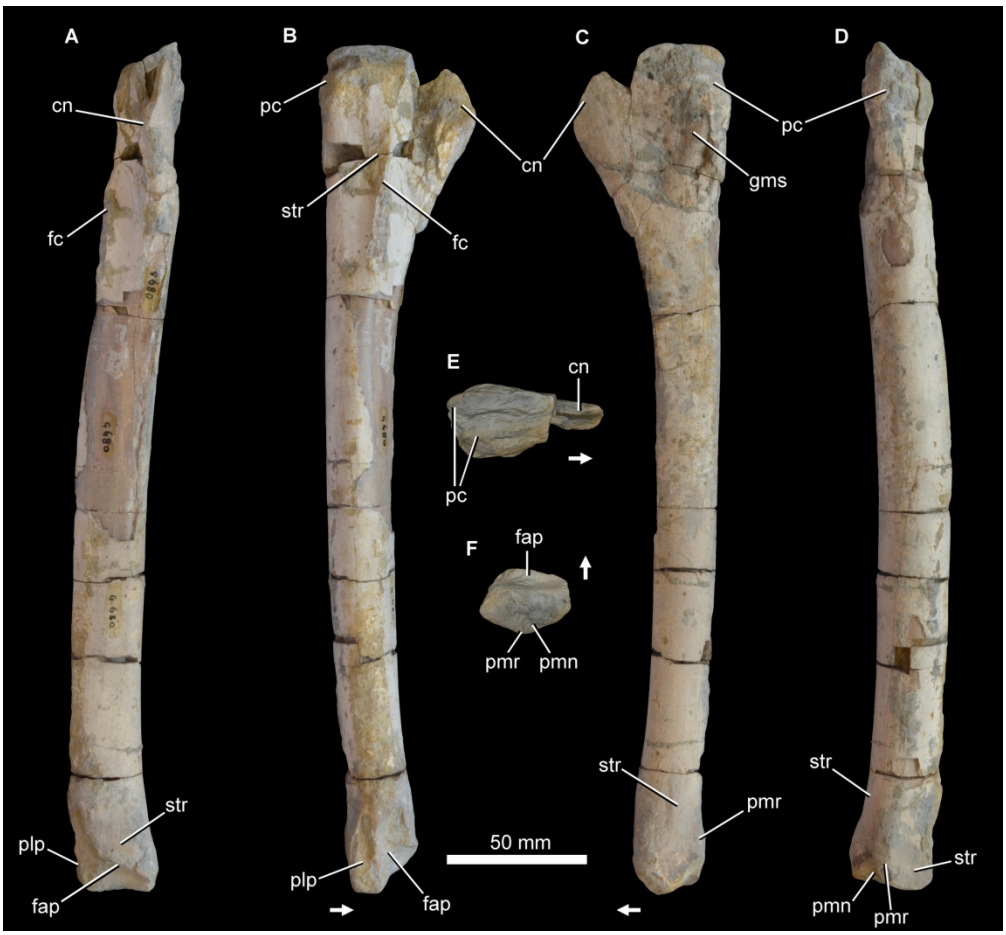

Figure 11. Right tibia of referred specimen of Sarcosaurus woodi, WARMS G680, in anterior (A), lateral (B), medial (C), posterior (D), proximal (E) and distal (F) views. Arrows point towards anterior direction. Abbreviations: cn, cnemial crest; fap, facet for reception of ascending process of astragalus; fc, fibular crest; gms, origin scar of the M. gastocnemius pars medialis; pc, posterior hemicondyles; plp, posterolateral process; pmn, posteromedial notch; pmr, posteromedial ridge; str, striations.

167x155mm (300 x 300 DPI)

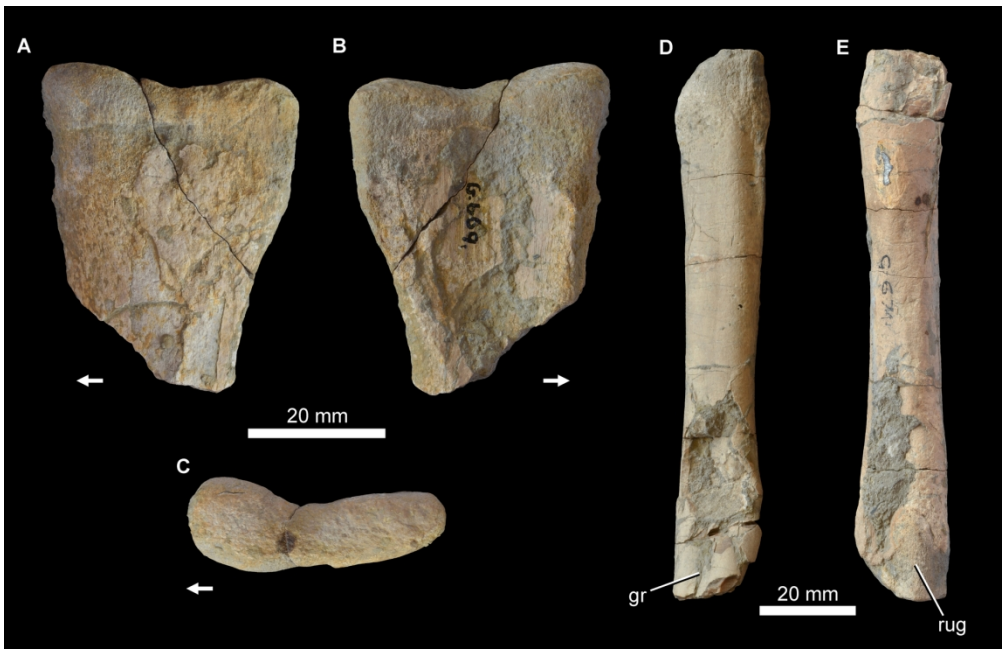

Figure 12. Fibula of referred specimen of Sarcosaurus woodi, WARMS G669 (A–C) and G674 (D, E). Proximal end of left fibula in lateral (A), medial (B) and proximal (C) views. Distal portion of fibula from indeterminate side in lateral/medial views (D, E). Arrows point towards anterior direction. Abbreviations: gr, groove; rug, rugosity.

167x108mm (300 x 300 DPI)

Figure 13. Partial left pedal autopodium (A–K) and metatarsal of indeterminate side (L) of referred specimen of Sarcosaurus woodi, WARMS G672 (A–C), G673 (D–F), G677 (G, H), G687 (I–K) and G671 (L). Metatarsal II in anterior (A), lateral (B) and distal (C) views. Metatarsal III in proximal (D), anterior (E) and lateral (F) views. Metatarsal IV in anterior (G) and lateral (H) views. Phalanx II-1 in anterior (I), proximal (J) and lateral (K) views. Proximal end of metatarsal II or III in lateral/medial view (L). Arrows point towards anterior direction. Abbreviations: clf, collateral fossa.

167x181mm (300 x 300 DPI)

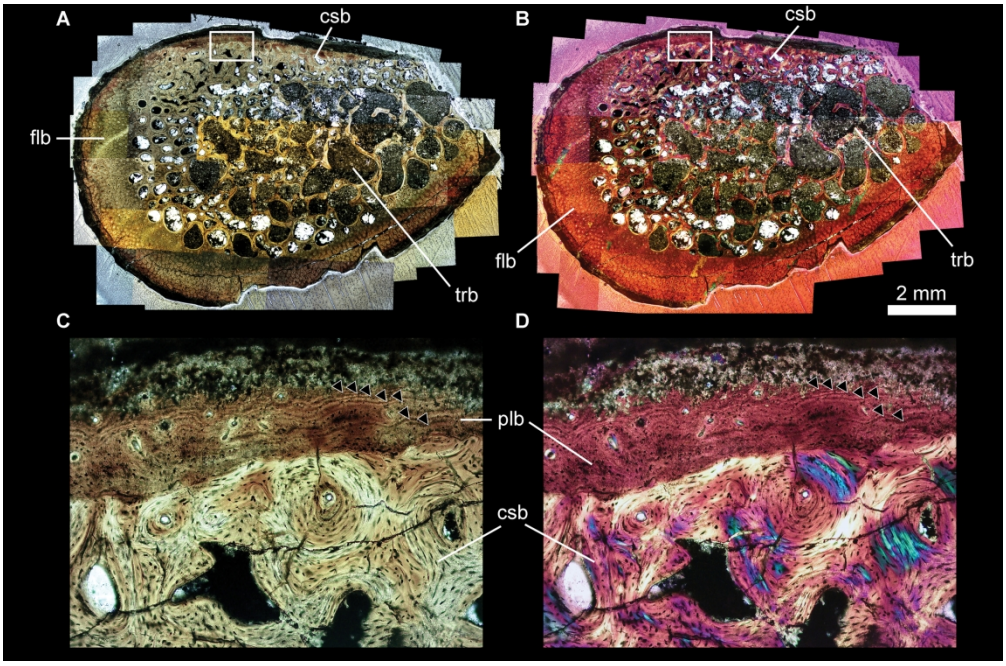

Figure 14. Photomicrographs of a thin section of dorsal rib shaft of referred specimen of Sarcosaurus woodi, WARMS G676, under plain-polarized light (A, C) and polarized light with a gypsum plate (B, D). White rectangles in (A, B) indicate the magnified areas shown in (C, D). Arrowheads in (C, D) indicate annuli. Abbreviations: csb, compact spongy bone; flb, fibrolamellar bone; plb, pseudolamellar bone; trb, trabeculae.

209x138mm (300 x 300 DPI)

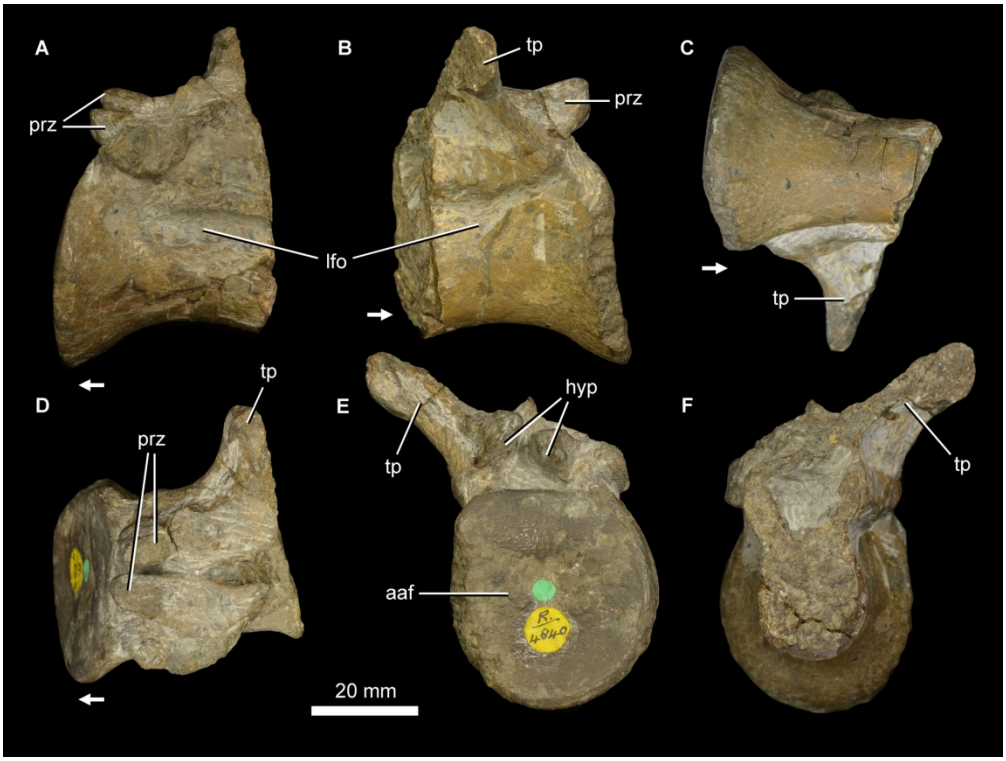

Figure 15. Posterior dorsal vertebra of holotype specimen of Sarcosaurus woodi, NHMUK PV R4840, in left lateral (A), right lateral (B), ventral (C), dorsal (D), anterior (E) and posterior (F) views. Arrows point towards anterior direction. Abbreviations: aaf, anterior articular facet; hyp, hypantrum; lfo, lateral fossa; prz, prezygapophysis; tp, transverse process.

167x126mm (300 x 300 DPI)

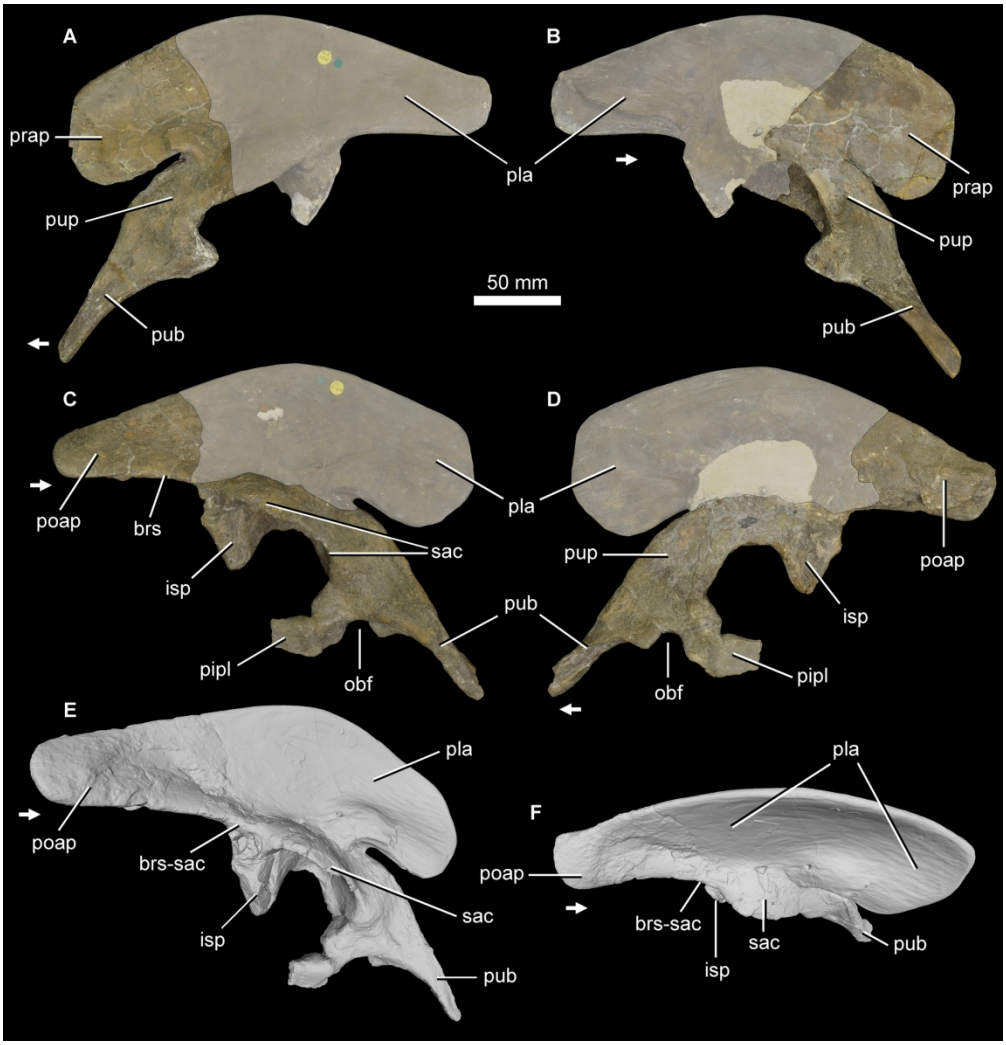

Figure 16. Partial pelvic girdle of holotype specimen of Sarcosaurus woodi, NHMUK PV R4840. Photographs (A–D) and surface scans (E, F) of left ilium and pubis (A, B) and right ilium and pubis (C–F) in lateral (A, C), medial (B, D), lateral and slightly posterior (E), and dorsal and slightly lateral (F) views. Arrows point towards anterior direction. Grey shaded regions are reconstructed. Abbreviations: brs, brevis shelf; brs-sac connection between brevis shelf and supraacetabular crest; isp, ischiadic peduncle; obt, obturator foramen; pipl, pubo-ischiadic plate; pla, plaster; poap, postacetabular process; prap, preacetabular process; pub, pubis; pup, pubic peduncle; sac, supraacetabular crest.

167x173mm (300 x 300 DPI)

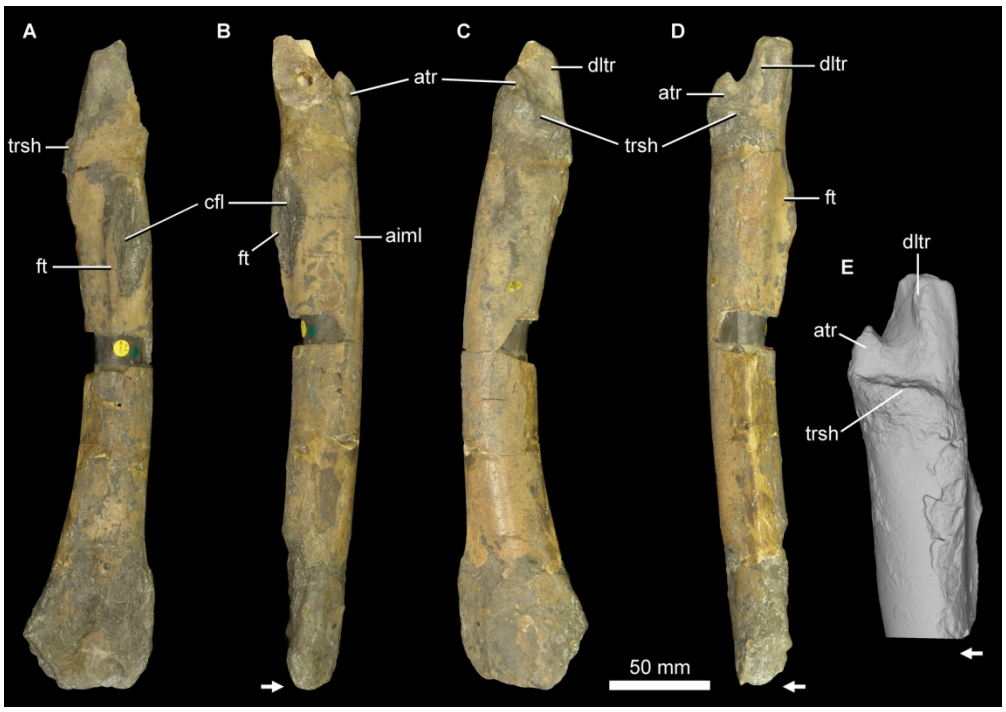

Figure 17. Left femur of holotype specimen of Sarcosaurus woodi, NHMUK PV R4840. Photographs (A–D) and surface scan (E) in posterior (A), medial (B), anterior (C), lateral (D), and lateral and slightly anterior (E) views. Arrows point towards anterior direction. Abbreviations: aiml, anterior intermuscular line; atr, anterior trochanter; cfl, depression associated with the insertion of the M. caudofemoralis longus; dltr, dorsolateral trochanter; ft, fourth trochanter; trsh, trochanteric shelf.

167x117mm (300 x 300 DPI)

Figure 18. Right tibia of referred specimen of Sarcosaurus woodi, NHMUK PV R3542 (holotype of 'Sarcosaurus andrewsi'). Photographs (A–F) and surface scan (G) in lateral (A), medial (B), anterior (C), posterior (D), proximal (E), distal (F), and medial and slightly anterior (G) views. Arrows point towards anterior direction. Abbreviations: adt, anterior diagonal tuberosity; cn, cnemial crest; fap, facet for reception of ascending process of astragalus; fc, fibular crest; mma, medial malleolus; pamr, paramarginal ridge; pc, posterior hemicondyles; plp, posterolateral process; pmn, posteromedial notch; pmr, posteromedial ridge.

167x149mm (300 x 300 DPI)

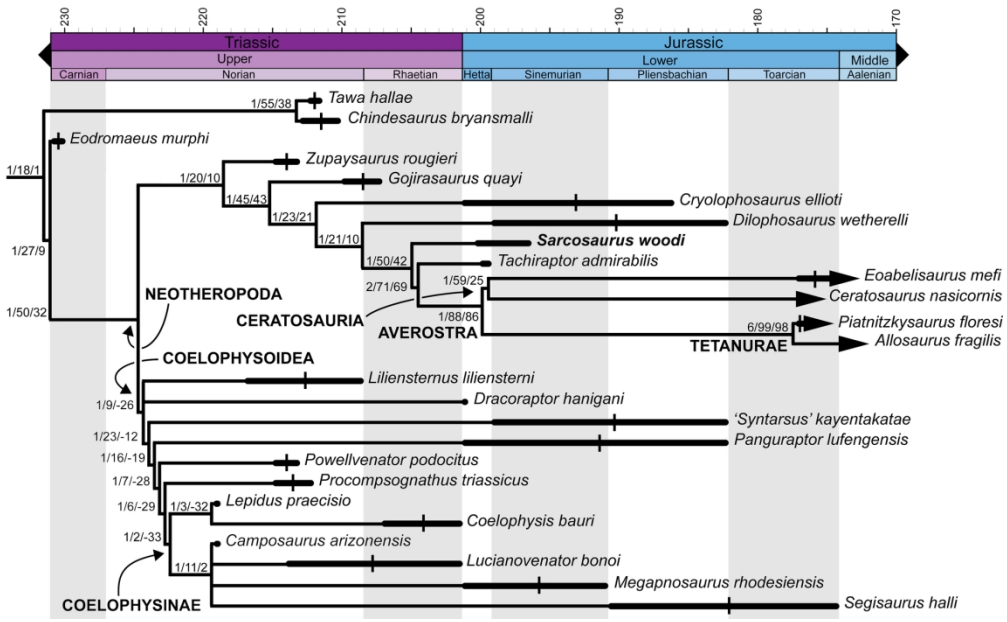

Figure 19. Time-calibrated strict consensus tree showing the phylogenetic relationships of selected non-neotheropod and all neotheropod species sampled in the phylogenetic analysis. Values next to each branch represent Bremer support, absolute bootstrap frequency, and GC bootstrap frequency, respectively. Thick black bars with a vertical line represent the chronostratigraphic uncertainty of taxa and thick black bars without a vertical line represent biochrons.

167x104mm (300 x 300 DPI)

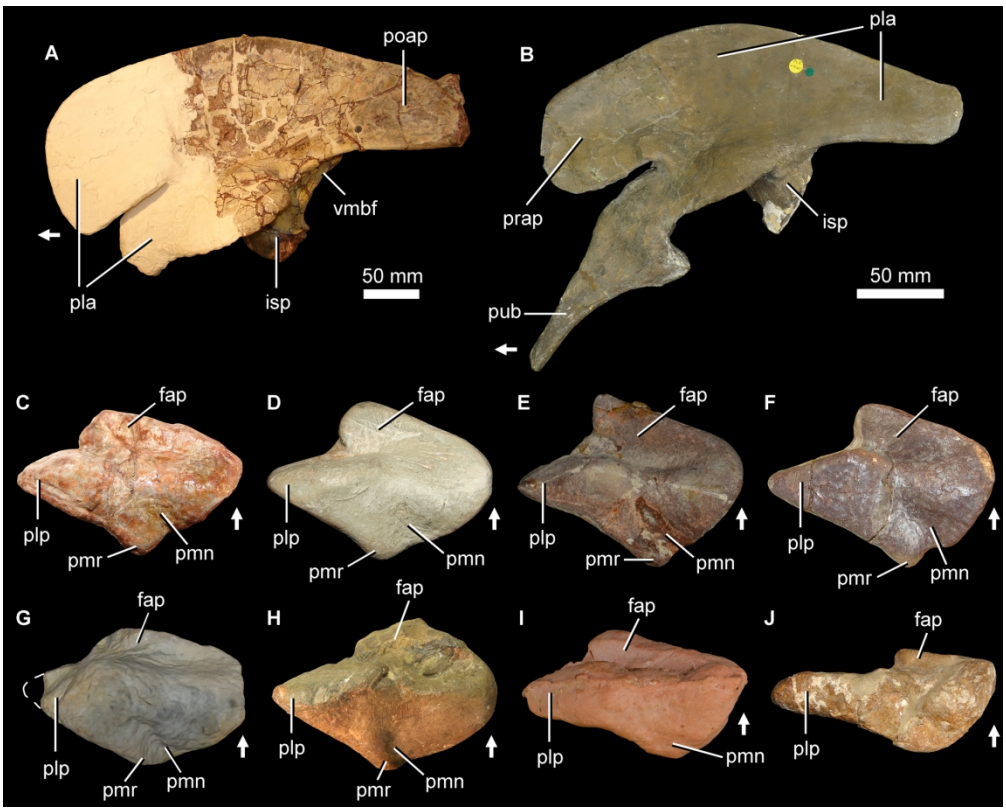

Figure 20. Comparison among partial ilia in lateral view (A, B) and tibiae in distal view (C–J) of selected neotheropod species. Dilophosaurus wetherilli (A, F), Sarcosaurus woodi (B, G, H), Coelophysis bauri (C), Liliensternus liliensterni (D), Zupaysaurus rougieri (E), Tachiraptor admirabilis (I) and Piatnitzkysaurus floresi (J). UCMP 37302 (A), NHMUK PV R4840 (B), AMNH unnumbered, reversed (C), HMN MB.R. 2175 (D), PULR 076 (E), UCMP 77270 (F), composite reconstruction using WARMS G668, 680 (G), NHMUK PV R3542 (H), LPRP/USP 0747, cast of IVIC-P-2867 (I) and MACN-Pv CH 895, reversed (J). Arrows point towards anterior direction. Abbreviations: fap, facet for reception of ascending process of astragalus; isp, ischiadic peduncle; pla, plaster; plp, posterolateral process; pmr, posteromedial ridge; pmn, posteromedial notch; poap, postacetabular process; prap, preacetabular process; pub, pubis; vmbf, ventromedial margin of brevis fossa. (C–J) Not to scale.

167x134mm (300 x 300 DPI)

Figure 21. Life reconstruction of the non-averostran neotheropod Sarcosaurus woodi from the late Hettangian–early Sinemurian of central England. Artwork by Mark Witton, who retains the copyright.

167x83mm (600 x 600 DPI)